

# RECIPE-TKG: From Sparse History to Structured Reasoning for LLM-based Temporal Knowledge Graph Completion

Anonymous ACL submission

## Abstract

Temporal Knowledge Graphs (TKGs) represent dynamic facts as timestamped relations between entities. While Large Language Models (LLMs) show promise for TKG completion, current approaches typically apply generic pipelines (neighborhood sampling, supervised fine-tuning, uncalibrated inference) without task-specific adaptation to temporal relational reasoning. Through systematic analysis under unified evaluation, we reveal three key failure modes: (1) retrieval strategies miss multi-hop dependencies when target entities are not directly observed in history, (2) standard fine-tuning reinforces memorization over relational generalization, and (3) uncalibrated generation produces contextually implausible entities. We present RECIPE-TKG, a parameter-efficient framework that addresses each limitation through principled, task-specific design: rule-based multi-hop sampling for structural grounding, contrastive fine-tuning to shape relational compatibility, and test-time semantic filtering for contextual alignment. Experiments on four benchmarks show that RECIPE-TKG outperforms prior LLM-based methods across input regimes, achieving up to 22.4% relative improvement in Hits@10, with particularly strong gains when historical evidence is sparse or indirect.

## 1 Introduction

Temporal Knowledge Graphs (TKGs) are widely used to represent dynamic, real-world knowledge across domains such as news (Boschee et al., 2015; Leetaru and Schrodt, 2013), biomedicine (Chaturvedi, 2024), and finance (Dukkipati et al., 2025). They capture facts as time-stamped relational tuples (subject, relation, object, timestamp), modeling how interactions evolve over time (Tresp et al., 2015). A core task in this setting is TKG completion,

The code is available at [this anonymous repository](#).

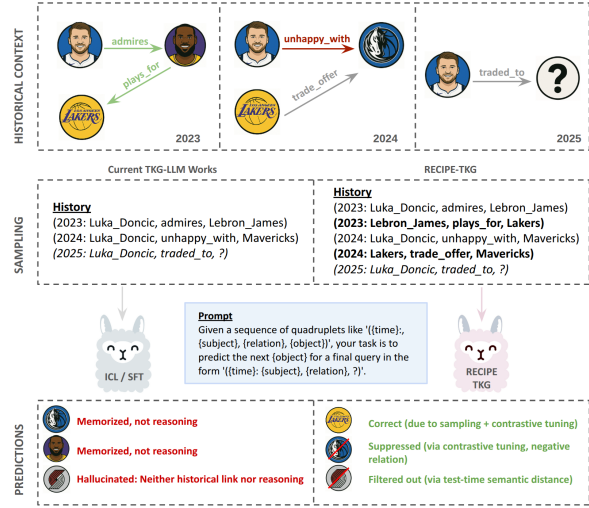


Figure 1: Example of LLM-based TKG reasoning. Pipelines that rely on one-hop context tend to prefer locally frequent or lexically similar entities, yielding off-context outputs. RECIPE-TKG augments history with structurally and temporally richer facts and applies semantic checking, producing more plausible predictions.

which involves predicting missing or future links based on observed temporal interactions. This task requires reasoning over both relational and temporal structure, with downstream applications in forecasting and decision support (Trivedi et al., 2017; Jin et al., 2020).

The rise of Large Language Models (LLMs) has sparked interest in using pretrained generative models for TKG completion, driven by their generalization capability and emergent reasoning skills (Liao et al., 2024; Luo et al., 2024; Lee et al., 2023). While LLM reasoning is often benchmarked on math or logic-based tasks (Lewkowycz et al., 2022; Wang et al., 2025), TKG completion provides a complementary testbed that emphasizes two challenges: (1) integrating temporal and structural signals beyond one-hop evidence, and (2) generalizing when history is *sparse* or the answer is *non-historical* (absent from retrieved context and typi-

001

002

003

004

005

006

007

008

009

010

011

012

013

014

015

016

017

018

019

020

021

022

023

024

025

026

027

028

029

030

031

032

033

034

035

036

037

038

039

040

041

042

043

044

045

046

047

048

049

050

051

052

053

054

055

056

057

058

059

060

061 cally reachable only via multi-hop paths).

062 Recent prompting-based and fine-tuned LLM  
063 methods (Lee et al., 2023; Liao et al., 2024; Luo  
064 et al., 2024; Xia et al., 2024a) report promising  
065 results. However, **these approaches typically adapt**  
066 **LLMs through generic pipelines** borrowed from  
067 other domains: shallow neighborhood sampling for  
068 context retrieval, standard supervised fine-tuning  
069 objectives, and uncalibrated inference at test time.  
070 This overlooks the unique characteristics of tem-  
071 poral relational reasoning, where answers often re-  
072 quire multi-hop inference over time-evolving struc-  
073 ture rather than surface pattern matching. As illus-  
074 trated in Figure 1, models frequently favor entities  
075 that are lexically similar or locally frequent in the  
076 input even when the graph structure supports better  
077 completions.

078 **Under a unified evaluation (Section 2), our**  
079 **analysis reveals three recurrent limitations.** (1)  
080 *Shallow retrieval* misses multi-hop, time-aligned  
081 evidence, which is crucial when the gold entity is  
082 not observed in history. (2) *Standard fine-tuning*  
083 primarily rewards token correctness and reinforces  
084 memorization rather than relational compatibility,  
085 with sharp drops on queries that require generaliza-  
086 tion beyond observed patterns. (3) *Uncalibrated in-  
087 ference* produces contextually implausible entities,  
088 often deviating from history without improving ac-  
089 curacy. These limitations indicate that task-specific  
090 design is necessary for effective LLM-based TKG  
091 completion.

092 We present **RECIPE-TKG**, a parameter-  
093 efficient framework that addresses each limi-  
094 tation with a principled, stage-wise design. (1)  
095 **Rule-Based Multi-Hop (RBMH) sampling** en-  
096 riches the retrieved history with structurally di-  
097 verse, temporally aligned facts to improve multi-  
098 hop reachability. (2) **Contrastive Fine-Tuning**  
099 (**CFT**) augments next-token prediction with a re-  
100 lational compatibility objective over LoRA adapters,  
101 encouraging discrimination among plausible can-  
102 didates rather than memorization of token patterns.  
103 (3) **Test-time semantic filtering** verifies con-  
104 textual alignment during inference and refines low-  
105 alignment outputs, reducing off-context predictions  
106 without additional training.

107 Across four benchmarks, RECIPE-TKG im-  
108 proves accuracy and plausibility, with especially  
109 strong gains in short-history and non-historical set-  
110 tings, and achieves up to **22.4%** relative improve-  
111 ment in Hits@10 over prior LLM-based methods.

## Contributions.

- We standardize evaluation to separate the effects of sampling, training, and inference, clarifying where reported gains originate.
- We provide a systematic characterization of failure modes in LLM-based TKG completion, centered on retrieval depth, supervision signal, and inference calibration.
- We introduce **RECIPE-TKG**, a task-specific, parameter-efficient framework whose stages directly target these limitations, yielding consistent gains across datasets and input regimes.

## 2 Unified Analysis of Failure Modes in LLM-based TKG Completion

Despite recent progress, LLMs adapted to TKG completion often default to surface patterns and fail when structural or temporal cues are indirect or require multi-hop reasoning. To guide design choices, we conduct a controlled re-evaluation of recent approaches (Lee et al., 2023; Liao et al., 2024) under a unified setup.

### 2.1 Grounding Predictions in Historical Context

#### Definition 2.1

A query’s history is **sparse** when the retrieved context contains few and/or low-diversity facts. A prediction is **non-historical** if the gold entity does not appear in the retrieved history prior to the query time. The notions overlap but are not identical.

Figure 2(a–c) provides three empirical facts that drive our design. (1) **History length matters:** Hits@10 is below 0.3 with only one retrieved fact and exceeds 0.5 with 20–50 facts, and this trend holds for both ICL and SFT (Fig. 2a). (2) **Structure, not just tokens:** over 25% of targets require multi-hop reachability and about 4% are unreachable with shallow sampling (Fig. 2b), indicating that merely adding more one-hop facts is insufficient. (3) **Non-historical collapse:** while LLMs achieve 80–83% Hits@10 on historical cases, accuracy falls below 5% when the gold entity is unseen in history (Fig. 2c), revealing a reliance on lexical overlap and pattern recall.

Taken together, these results point to *depth and temporal alignment in history sampling*, rather than

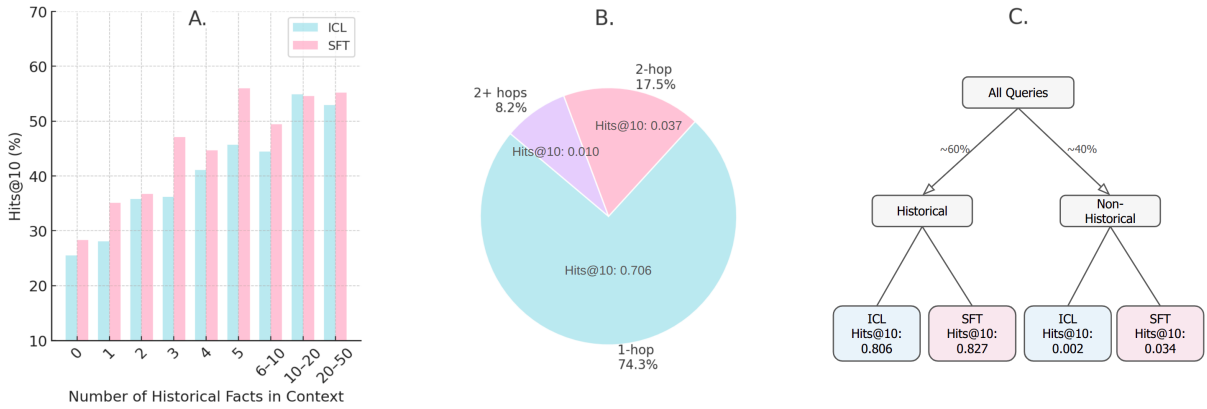


**Figure 2: Failures under short history and non-historical answers.** Dataset: ICEWS14. Model: LLaMA-2-7B. (a) Hits@10 vs. number of retrieved facts (history length): longer histories support better reasoning. (b) Share of queries by minimum hop distance from subject to gold entity: over 25% require multi-hop reachability. (c) Hits@10 by historical (gold seen in retrieved history) vs. non-historical (gold unseen) splits for ICL and SFT, showing a sharp drop in the latter.

longer but shallow context, as the primary driver of accuracy. They motivate a mitigation that (i) recovers multi-hop, time-aligned evidence and (ii) trains for *relational compatibility* beyond memorized associations. We operationalize this in Section 4 via multi-hop, graph-aware history sampling and CFT that encourages such compatibility.

## 2.2 Limitations of Supervised Fine-Tuning

Table 1: Re-evaluation of ICL and SFT using consistent decoding and evaluation. Gains largely stem from evaluation setup and history sampling; the marginal effect of SFT is smaller under a unified setup.

Method	Hits@1	Hits@3	Hits@10
<i>Reported in GenTKG</i>			
ICL (naive sampling + basic eval)	0.258	0.430	0.510
+ Fine-Tuning (TLR sampling + eval)	0.369	0.480	0.535
<i>Re-evaluated under consistent setup</i>			
ICL (naive sampling) + GenTKG eval	0.344	0.464	0.523
ICL (TLR sampling) + GenTKG eval	0.351	0.473	0.527
SFT (TLR sampling) + GenTKG eval	0.364	0.476	0.532

Supervised fine-tuning (SFT) is widely used to adapt LLMs to TKG tasks, and prior work such as GenTKG (Liao et al., 2024) reports notable improvements over prompting-based strategies (Lee et al., 2023). However, our re-evaluation under controlled conditions shows that much of this improvement originates not from fine-tuning itself, but from differences in sampling strategies and evaluation setups.

**Evaluation Frameworks Explain Much of the Gap.** LLMs produce open-ended text that requires careful postprocessing to extract valid entity predictions. While Lee et al. (2023) uses a basic evaluation setup, GenTKG applies a more refined

pipeline with canonicalization and output filtering, making direct comparisons misleading.

To disentangle these effects, we re-evaluate prompting-based strategies and fine-tuned models with different sampling and evaluation pipelines under a unified framework. We compare naive sampling used in Lee et al. (2023) and TLR sampling (Liao et al., 2024), and two evaluation settings (basic eval and GenTKG eval (Liao et al., 2024)). As shown in Table 1, replacing the evaluation code alone increases Hits@1 from 25.8% to 34.4%. TLR sampling provides a modest improvement (35.1%) compared to one-hop sampling, while fine-tuning adds only a small additional gain (36.4%). This suggests that a large portion of the reported gain stems from implementation choices, not from the model’s improved reasoning capabilities.

**Fine-tuning alone does not fix generalization.** As established in Section 2.1, both ICL and fine-tuned models struggle with non-historical predictions, where the correct answer does not appear in the retrieved history. These failures persist across a range of input sizes and are especially severe when the gold entity requires multi-hop reasoning, which is not supported by current sampling methods. Fine-tuning improves memorization of patterns seen during training but does not provide the relational inductive bias needed to reason about unseen or indirectly connected entities.

**Motivating contrastive fine-tuning.** We therefore supplement next-token prediction with a contrastive objective that explicitly separates plausible from implausible candidates conditioned on relations, encouraging compatibility-driven discrimination under sparse or indirect evidence (Section 4).

153  
154  
155  
156  
157  
158  
159  
160

161  
162  
163  
164  
165  
166  
167  
168  
169

170  
171  
172  
173  
174

175  
176  
177  
178  
179  
180  
181  
182  
183  
184  
185  
186  
187  
188  
189  
190  
191  
192  
193  
194  
195  
196  
197  
198  
199  
200  
201  
202  
203  
204  
205  
206  
207  
208  
209

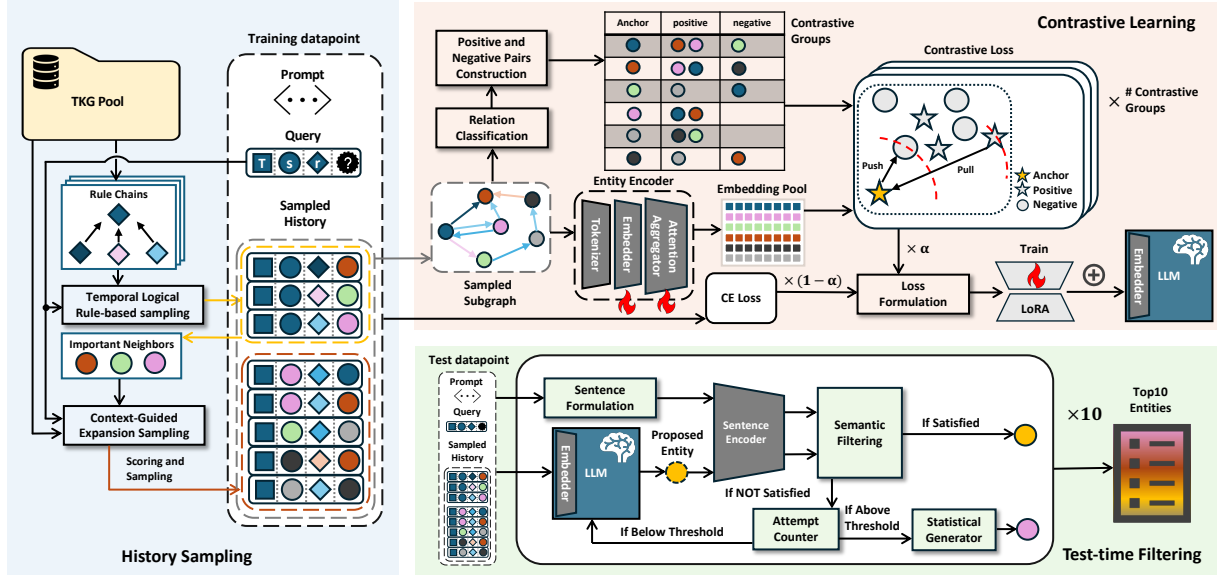


Figure 3: **Overview of RECIPE-TKG.** RECIPE-TKG follows a three-stage framework: (1) **History Sampling**, which retrieves query-relevant facts via a two-phase strategy combining rule-based retrieval and context-guided expansion; (2) **Contrastive Learning**, which jointly optimizes entity embeddings using contrastive and cross-entropy losses. Positive/negative pairs are sampled from the subgraph, and embeddings are generated via a learnable encoder; (3) **Test-time Filtering**, where predicted entities are iteratively verified by a semantic filter. Unsatisfactory outputs are refined using a statistical generator until confident predictions are obtained.

### 3 Preliminaries

**Problem Formulation.** A Temporal Knowledge Graph is a collection of time-stamped facts represented as quadruples  $(s, p, o, t)$ , where  $s$  and  $o$  are subject and object entities,  $p$  is a relation, and  $t$  denotes the timestamp of the event. Formally, a TKG is denoted as  $\mathcal{G} = (\mathcal{V}, \mathcal{R}, \mathcal{E}, \mathcal{T})$ , where  $\mathcal{V}$  is the set of entities,  $\mathcal{R}$  the relations,  $\mathcal{E}$  the event facts, and  $\mathcal{T}$  the time indices. Each time step  $t$  defines a historical snapshot  $\mathcal{G}_t \subseteq \mathcal{E}$ . The forecasting task involves predicting a missing entity in a future quadruple. Given a query of the form  $(s, p, ?, t)$  or  $(?, p, o, t)$  and a set of historical snapshots  $\{\mathcal{G}_1, \dots, \mathcal{G}_{t-1}\}$ , the model must return the most plausible entity that completes the query at time  $t$ .

**Low-Rank Adaptation (LoRA)** To reduce the number of trainable parameters, we adopt LoRA (Hu et al., 2022), which re-parameterizes the weight update as % %

$$\hat{h}(x) = W_0 x + A B x, \quad (1)$$

where  $W_0$  is a frozen pretrained weight and  $A, B$  are trainable low-rank matrices.

### 4 Method

In this section, we present RECIPE-TKG, a three-stage LLM-based lightweight (see Appendix B) framework for temporal knowledge forecasting. The complete framework is illustrated in Figure 3.

#### 4.1 RBMH: Rule-Based Multi-Hop History Sampling

The first stage of RECIPE-TKG focuses on retrieving a compact yet informative history from the temporal knowledge graph  $\mathcal{G}$ . For a given query  $(s_q, p_q, ?, T)$ , we aim to retrieve historical facts  $\{(s, p, o, t) \in \mathcal{G} \mid t < T\}$  that are temporally valid and structurally relevant. Our sampling process combines rule-based retrieval with context-guided expansion to provide richer support for reasoning, particularly in sparse or non-historical settings.

**Stage 1: Temporal Logical Rule-based Sampling.** We begin by retrieving subject-aligned 1-hop facts using a rule-based procedure adapted from TLR (Liao et al., 2024), which learns relational rules of the form  $p_q \Leftarrow \{p_{b_1}, \dots, p_{b_k}\}$  through 1-step temporal random walks, capturing event regularities. We retrieve historical quadruples  $(s, p, o, t)$  such that  $s = s_q$  and  $p$  appears in the rule body for the query relation  $p_q$ . See Appendix A.1 for the details.

However, this 1-hop retrieval cannot reach facts involving semantically relevant but structurally distant entities. Due to the fixed number of learned rules, this stage often retrieves fewer than  $N$  quadruples, the maximum the LLM can handle. This motivates a second stage to expand context with more diverse and informative facts.

265 **Stage 2: Context-guided Multi-hop Expansion**

266 We then sample additional historical facts from  
 267  $\mathcal{G}$ . The candidate pool includes any quadruples not  
 268 retrieved in Stage 1 whose subjects differ from  $s_q$ .

269 This stage is designed to support multi-hop reasoning by identifying facts that may not directly  
 270 connect to the query subject but are structurally and  
 271 semantically relevant. Each candidate  $(s, p, o, t)$  is  
 272 assigned a composite weight:

274 
$$w = w_n \cdot w_f \cdot (w_t + w_c + w_{cp}), \quad (2)$$

275 where  $w_n$  downweights unreachable or distant  
 276 nodes,  $w_f$  penalizes high-frequency triples,  $w_t$  priori-  
 277 tizes temporal recency,  $w_c$  favors co-occurrence  
 278 with the query subject or relation, and  $w_{cp}$  rein-  
 279 forces connectivity with the initial TLR context.

280 To sample from candidate pool, We first select  
 281 the top  $10 \times M$  candidates by score to form a re-  
 282duced pool, where  $M$  is the context window bud-  
 283 get. From this pool, we sample  $M$  quadruples with  
 284 probabilities proportional to their weights. This  
 285 soft filtering strategy preserves diversity while pri-  
 286 oritizing high-quality candidates, avoiding over-  
 287 reliance on only the highest-scoring facts. Our two-  
 288 stage RBMH sampling method supports reasoning  
 289 beyond immediate neighbors and avoids overfitting  
 290 to shallow or overly common facts. The overall  
 291 design motivation, formal definitions, hyperparam-  
 292 eters and algorithms are provided in Appendix A.2.

293 **4.2 Contrastive Fine-Tuning for Structured**  
 294 **Reasoning**

295 To improve generalization beyond memorized en-  
 296 tity associations, we introduce a contrastive fine-  
 297 tuning objective that supplements the standard next-  
 298 token prediction loss, helping to disambiguate plau-  
 299 sible from implausible predictions, especially when  
 300 historical context is sparse or indirect.

301 **Relation-Guided Contrastive Pair Construction.**  
 302 Our design is guided by the international relations  
 303 principle, *The enemy of my enemy is my friend*,  
 304 which reflects relational patterns common in geo-  
 305 political TKGs and motivates how we position enti-  
 306 ties in embedding space. Inspired by this structure,  
 307 we first categorize relations into **positive**, **ne-  
 308 gative**, and **neutral** types using GPT-4o, minimiz-  
 309 ing the inclusion of neutral cases (see Appendix C.1).  
 310 Given a sampled subgraph (Figure 3), we treat each  
 311 unique entity as an anchor and examine its 1-hop  
 312 neighbors. A neighbor is assigned as a *positive*  
 313 sample if it connects via a positive relation, or a

negative sample if it connects via a negative relation.  
 314 If both types of edges exist, the neighbor is  
 315 excluded to avoid contradiction. Neutral relations  
 316 are ignored. This process forms contrastive groups  
 317 that are used to calculate the contrastive loss.  
 318

319 **Entity Embedding Encoding.** Since an entity  
 320 typically spans multiple tokens, we adopt a multi-  
 321 stage process to compute its representation. First,  
 322 the entity string is tokenized. Each resulting token  
 323 is then passed through the model’s embedding layer  
 324 (embedder), which produces an embedding vector.  
 325 These token embeddings  $\{h_1, h_2, \dots, h_k\}$  are sub-  
 326 sequently aggregated into a single entity-level em-  
 327 bedding  $e$  using a trainable **attention aggregator**.  
 328

The final embedding is a weighted sum:

$$e = \sum_{j=1}^k \lambda_j h_j, \quad (3)$$

330 where  $\lambda_j$  are attention weights satisfying  $\sum_j \lambda_j =$   
 331 1. Both the embedding layer and the aggregator  
 332 are learnable modules, jointly optimized during  
 333 fine-tuning.

334 **Training Objective.** The overall loss function is  
 335 defined as:

$$\mathcal{L} = \alpha \cdot \mathcal{L}_{\text{contrastive}} + (1 - \alpha) \cdot \mathcal{L}_{\text{ce}}(o, o_p), \quad (4)$$

336 where  $\mathcal{L}_{\text{ce}}$  denotes the cross-entropy loss between  
 337 the predicted token  $o_p$  and the ground truth  $o$ ,  
 338  $\mathcal{L}_{\text{contrastive}}$  represents the contrastive loss, and  $\alpha \in$   
 339  $[0, 1]$  is a balancing hyperparameter.

340 The contrastive loss is formulated as:

$$\mathcal{L}_{\text{contrastive}} = \frac{1}{N_c} \sum_{i=1}^{N_c} \max \left( 0, \right. \\ \left. \|a_i - pos_i\|^2 - \|a_i - neg_i\|^2 + m \right) \quad (5)$$

341 where  $N_c$  is the number of contrastive groups,  
 342 and  $a_i$  denotes the embedding of the anchor entity.  
 343 For each group,  $pos_i$  is the hardest positive, defined  
 344 as the farthest positive entity from the anchor in the  
 345 embedding space, while  $neg_i$  is the closest negative.  
 346 This formulation emphasizes challenging examples  
 347 and enforces a margin  $m$  to improve the separation  
 348 between positive and negative pairs.

349 This training objective encourages the model  
 350 to pull the most distant positive samples closer to  
 351 the anchor and push the nearest negatives farther  
 352 away. This dynamic adjustment refines the semantic  
 353 structure of the latent space, enabling better  
 354

entity discrimination and improving downstream reasoning performance. More details can be found at Appendix C.

### 4.3 Similarity-Based Test-Time Filtering

Recent work shows that language models can improve inference without parameter updates by using lightweight test-time strategies (Snell et al., 2024; Ji et al., 2025). Building on this idea, we introduce a semantic similarity-based filtering method to reduce hallucinations by removing predictions misaligned with the input context.

Our filtering approach is motivated by two empirical observations:

1. Models often generate non-historical entities that have low semantic alignment with the input context, especially in sparse settings despite higher similarity scores correlating with correctness (Figure 4).
2. In many cases, the ground truth entity already appears in the historical context  $\mathcal{H}$ , yet the model produces a non-historical prediction that yields negligible gain in accuracy.

These patterns suggest that enforcing semantic consistency and reconsidering salient entities from the input can correct many low-quality predictions. Rather than rejecting or reranking predictions with fixed rules, we apply an adaptive refinement strategy grounded in semantic similarity.

**Semantic Consistency Verification.** We embed the generated prediction  $p$  and the input context  $c$  using a sentence transformer model to compute a similarity score:

$$\phi(p, c) = \text{cos-sim}(E(p), E(c)) \quad (6)$$

$$E(x) = \text{SentenceTransformer}(x) \in \mathbb{R}^d \quad (7)$$

where  $E(\cdot)$  denotes the output vector of a pre-trained transformer model. We use this similarity as a proxy for contextual alignment. A prediction is accepted if its similarity score exceeds a learned threshold  $\tau$ , or if it already appears in the retrieved history  $\mathcal{H}$ . Otherwise, we regenerate until a satisfactory prediction is found, or fall back to history-aware scoring.

This process is formalized as:

$$p' = \begin{cases} p & \text{if } p \in \mathcal{H} \text{ or } \phi(p, c) \geq \tau \\ \text{regenerate}(p) & \text{if } \phi(p, c) < \tau \\ \arg \max_{h \in \mathcal{H}} \psi(h) & \text{after } k \text{ attempts} \end{cases} \quad (8)$$

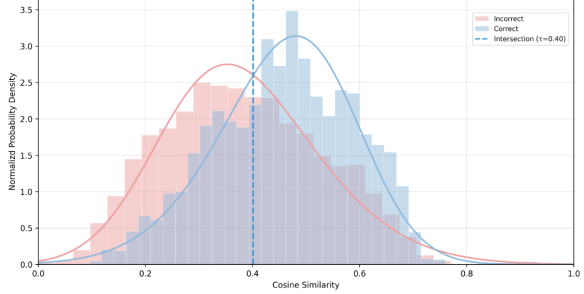


Figure 4: Distribution of semantic similarity values for correctly and incorrectly classified samples to the input context.

Figure 3 illustrates how filtering interacts with the generation process to improve robustness.

**Historical Relevance Fallback.** If repeated generations yield unsatisfactory predictions, we fall back to the historical candidates  $\mathcal{H}$ . Each candidate  $h \in \mathcal{H}$  is scored by:

$$\psi(h) = \beta \cdot f(h) + (1 - \beta) \cdot r(h) \quad (9)$$

where  $f(h)$  is the frequency of  $h$  in the input history and  $r(h)$  captures recency. This mechanism biases the selection toward historically grounded entities when semantic alignment fails.

**Threshold Selection.** The threshold  $\tau$  is optimized to best separate correct and incorrect predictions based on empirical distributions of  $\phi(p, c)$ . We describe the optimization objective and quantitative justification in Appendix D, along with implementation details and discuss its generalizability in Appendix E.

## 5 Experiments

### 5.1 Experimental Setup

**Proposed method.** We refer to our full method as RECIPE-TKG, which combines rule-based multi-hop history sampling (*RBMH Sampling*), contrastive fine-tuning denoted as *CFT*, and *Test-time Filtering*.

**Language Models.** Our primary experiments are conducted on LLaMA-2-7B (Touvron et al., 2023), a widely used open-source model in LLM-based TKG completion research (Liao et al., 2024; Luo et al., 2024). To ensure modern relevance, we also evaluate LLaMA-3-8B (Meta AI, 2024). Prompts and implementation details are provided in Appendix C.2 and C.4

Table 2: **Temporal link prediction results on temporal-aware filtered Hits@1/3/10.** LLM-based models are implemented based on LLaMA2-7B. Best results for each metric are highlighted in **bold**, and the best results among LLM-based models are underlined. The last row shows the relative improvement ( $\Delta$ ) of RECIPE-TKG over the best-performing LLM-based baseline.

Datasets Models	ICEWS14			ICEWS18			GDELT			YAGO		
	Hits@1	Hits@3	Hits@10	Hits@1	Hits@3	Hits@10	Hits@1	Hits@3	Hits@10	Hits@1	Hits@3	Hits@10
Embedding-based	RE-NET (Jin et al., 2020)	0.260	0.401	0.548	0.165	0.297	0.447	<b>0.117</b>	0.202	0.333	-	-
	RE-GCN (Li et al., 2021)	0.313	0.473	0.626	0.223	0.367	<b>0.525</b>	0.084	0.171	0.299	0.468	0.607
	xERTE (Han et al., 2020)	0.330	0.454	0.570	0.209	0.335	0.462	0.085	0.159	0.265	0.561	0.726
	TANGO (Han et al., 2021)	0.272	0.408	0.550	0.191	0.318	0.462	0.094	0.189	0.322	0.566	0.651
Rule-based	TimeTraveler (Sun et al., 2021)	0.319	0.454	0.575	0.212	0.325	0.439	0.112	0.186	0.285	0.604	0.770
	TLogic (Liu et al., 2022)	0.332	0.476	0.602	0.204	0.336	0.480	0.113	<b>0.212</b>	<b>0.351</b>	0.638	0.650
LLM-based	CoH (Xia et al., 2024b)	0.242	0.397	0.512	0.168	0.282	0.427	-	-	-	-	-
	PPT (Xu et al., 2023)	0.289	0.425	0.570	0.169	0.306	0.454	-	-	-	-	-
	HFL (Xu et al., 2025)	0.277	0.427	0.573	0.178	0.304	0.455	-	-	-	-	-
	ICL (Lee et al., 2023)	0.344	0.464	0.523	0.164	0.302	0.382	0.090	0.172	0.242	0.738	0.807
	GenTKG (Liao et al., 2024)	0.364	0.476	0.532	0.200	0.329	0.395	<u>0.099</u>	<u>0.193</u>	0.280	0.746	0.804
RECIPE-TKG		<b>0.393</b>	<b>0.526</b>	<b>0.651</b>	<b>0.224</b>	<b>0.369</b>	<b>0.516</b>	0.095	0.192	0.327	<b>0.811</b>	<b>0.880</b>
$\Delta$		8.0%	10.5%	22.4%	12.0%	12.2%	13.4%	-4.0%	-0.5%	16.8%	8.7%	9.0%

**Datasets.** We evaluate RECIPE-TKG on four commonly adopted benchmark datasets: ICEWS14 and ICEWS18, both derived from the ICEWS project (Boschee et al., 2015), GDELT (Leetaru and Schrodt, 2013), and YAGO (Mahdisoltani et al., 2013). Detailed dataset statistics are provided in Appendix H.

**Evaluation Metrics.** We choose temporal-aware filtered Hits@1/3/10 as our evaluation metrics, following prior work (Gastinger et al., 2023).

**Baselines.** We compare RECIPE-TKG against three categories of methods. **Embedding-based methods** include RE-NET (Jin et al., 2020), RE-GCN (Li et al., 2021), xERTE (Han et al., 2020), TANGO (Han et al., 2021), and TimeTraveler (Sun et al., 2021). **Rule-based method** includes TLogic (Liu et al., 2022). **LLM-based methods** include ICL (Lee et al., 2023), GenTKG (Liao et al., 2024), PPT (Xu et al., 2023), CoH (Xia et al., 2024b), and HFL (Xu et al., 2025). Additional information about baselines are in Appendix G.

## 5.2 Main Results

Results in Table 2 show that RECIPE-TKG consistently performs well across four benchmarks, surpassing both embedding-based and LLM-based baselines on nearly all evaluation metrics. On ICEWS14 and YAGO, RECIPE-TKG establishes new state-of-the-art results among LLM-based methods, achieving up to **22.4%** relative improvement in Hits@10. On ICEWS18, it exceeds the best LLM-based baseline on all three metrics and is competitive with RE-GCN, the strongest embedding-based model. For GDELT, which is known to be noisy and dominated by repetitive

Table 3: **Ablation study on ICEWS14 with LLaMA2-7B.** Comparison of training paradigms across different history sampling strategies. The bold results show the original combinations of components in prior works and our method.

	ICL			SFT			CFT		
	H@1	H@3	H@10	H@1	H@3	H@10	H@1	H@3	H@10
Lee et al. (2023)	<b>0.344</b>	<b>0.464</b>	<b>0.523</b>	0.360	0.469	0.530	0.363	0.479	0.529
TLR (Liao et al., 2024)	0.351	0.473	0.527	<b>0.364</b>	<b>0.476</b>	<b>0.532</b>	0.367	0.476	0.532
RBMH	0.364	0.500	0.572	0.389	0.519	0.582	<b>0.392</b>	<b>0.521</b>	<b>0.580</b>

event patterns (Trivedi et al., 2017; Li et al., 2021) with fine-grained 15-minute timestamps that favor symbolic rule chaining, frequent rules can be mined reliably and simple chains often suffice, explaining TLogic’s advantage (Liu et al., 2022); nevertheless, RECIPE-TKG attains the highest Hits@10 (0.327) among LLM-based models and remains competitive on Hits@1 and Hits@3. These results highlight the effectiveness of RECIPE-TKG and position LLM-based methods as strong candidates for foundation models in TKG completion.

## 6 Analysis

### 6.1 Ablation Study

We conducted ablation studies to evaluate key components of our framework against prior works. We compare three sampling methods (Lee et al. (2023), TLR (Liao et al., 2024), and our *RBMH Sampling*) and three training paradigms (in-context learning, supervised fine-tuning, and contrastive fine-tuning) on ICEWS14 using LLaMA2-7B. As shown in Table 3, bold results indicate original combinations from prior works and RECIPE-TKG w/o filtering. The results show that *RBMH Sampling* consistently improves performance across all training paradigms by retrieving structurally diverse and se-

Table 4: Effect of removing RECIPE-TKG components.

SETTINGS	Hits@1	Hits@3	Hits@10
RECIPE-TKG w/o CFT	0.364	0.501	0.643
RECIPE-TKG w/o RBMH Sampling	0.364	0.483	0.581
RECIPE-TKG w/o Filtering	0.392	0.521	0.580
RECIPE-TKG	0.393	0.526	0.651

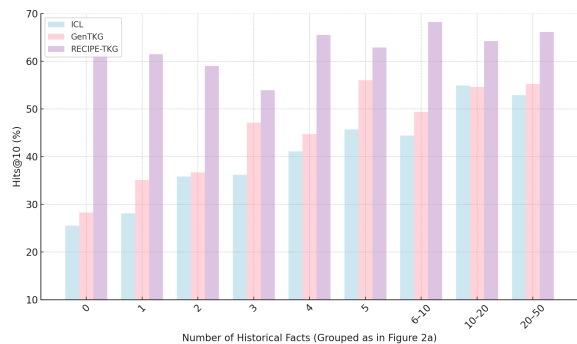


Figure 5: Hits@10 grouped by number of historical facts. RECIPE-TKG consistently outperforms ICL and GenTKG across all history lengths, with particularly strong improvements when the input history is sparse.

493  
494  
495  
496  
497  
498  
499  
500  
501  
502  
503  
504  
505  
506  
507  
508  
509  
510  
511

mantically relevant context. While *CFT* performs comparably to *SFT* with the same sampling strategy, it shows clear advantages when historical context is sparse. As discussed in Appendix I.1, contrastive models generate predictions semantically closer to the ground truth, even when exact matches aren’t possible, promoting structure-aware generalization beyond surface-level accuracy, especially in sparse settings where lexical cues are insufficient.

503  
504  
505  
506  
507  
508  
509  
510  
511

Table 4 provides additional insights into the effects of each of the three components, especially *test-time filtering*. When comparing the CFT-RBMH setting with and without *Test-time Filtering*, we observe a substantial boost in Hits@10 from 0.580 to 0.651, underscoring the effectiveness of our test-time refinement mechanism. Notably, combining *test-time filtering* with *RBMH Sampling* and *Test-time Filtering* (**RECIPE-TKG**) yields the best performance across all metrics.

## 512 6.2 Performance Gains Across Input Regimes

513  
514  
515  
516  
517  
518  
519  
520  
521  
522  
523

To evaluate how historical input affects model performance, we group queries by the number of retrieved facts and compare Hits@10 across methods. These bins align with Figure 2(a), allowing direct comparison with prior failure patterns. As shown in Figure 5, RECIPE-TKG outperforms both ICL and GenTKG across all groups, with especially large gains in the low-history regime.

Two key insights emerge. First, prior failures on short-history queries were not due to intrinsic difficulty, but rather to shallow retrieval. Since all

Table 5: Comparison between LLaMA2-7B and LLaMA3-8B on ICEWS14.

Model	LLaMA2-7B			LLaMA3-8B		
	hit@1	hit@3	hit@10	hit@1	hit@3	hit@10
ICL	0.344	0.464	0.523	0.351	0.484	0.578
RECIPE-TKG	0.393	0.526	0.651	0.367	0.529	0.658

524  
525  
526  
527  
528  
529  
530  
531

methods are evaluated on the same query set, the strong gains from RECIPE-TKG (reaching over 60% Hits@10 for history length 0 to 2) indicate that even sparse queries can be completed accurately when provided with deeper, multi-hop context. This validates the effectiveness of *RBMH Sampling* in recovering structurally and temporally relevant support.

532  
533  
534  
535  
536  
537

Second, RECIPE-TKG continues to outperform baselines even with longer histories (10–50 facts), where other methods begin to plateau. This sustained advantage reflects the contributions of *CFT* and *Test-time Filtering*, which improve generalization and reduce hallucinations.

538  
539  
540  
541

Overall, these results show that RECIPE-TKG not only addresses the limitations of shallow context but also improves reasoning and prediction quality across a wide range of query types.

## 542 6.3 Case Study: Performance of Llama3-8b

543  
544  
545  
546  
547  
548  
549  
550

As shown in Table 5, LLaMA3-8B performs comparably to LLaMA2-7B, supporting our choice of the latter for most experiments. Moreover, this choice of base model enables a fair comparison with prior work using fine-tuned models. Under both backbones, RECIPE-TKG consistently outperforms ICL, demonstrating its robustness and generalizability across different LLMs.

551  
552  
553  
554

**Lightweight design.** We update only  $\sim 0.81\%$  of LLaMA-2-7B (54.3M params), mine rules in  $<20$ s per dataset, and incur a 16.6% inference overhead from filtering (details in Appendix B).

## 555 7 Conclusion

556  
557  
558  
559  
560  
561  
562  
563  
564  
565

We introduced RECIPE-TKG, a framework for LLM-based temporal knowledge graph forecasting that combines multi-hop sampling, contrastive fine-tuning, and semantic filtering. It delivers consistent accuracy gains, especially under sparse or indirect evidence in practice. By aligning context with relational structure and refining inference, RECIPE-TKG improves reasoning without large-scale retraining, validating a modular, temporally grounded design overall.

566

## Limitations

567 Although RECIPE-TKG adopts a structured three-  
 568 stage framework, it is still built on clean, fully  
 569 observed temporal knowledge graphs, which may  
 570 not reflect real-world scenarios. The rule mining  
 571 step requires offline learning before sampling, and  
 572 must be repeated if the TKG changes. Moreover,  
 573 the framework assumes full observability of histori-  
 574 cal events, while in practice, such information may  
 575 be incomplete or noisy. Future work may explore  
 576 more robust designs that support dynamic updates  
 577 and reasoning under partially observed histories.

578 **License and Ethics**

579 All datasets used in this study are publicly available  
 580 and licensed for academic research. Specifically,  
 581 ICEWS14, ICEWS18, GDELT, and YAGO have  
 582 been widely adopted in prior work on temporal  
 583 knowledge graphs. No personally identifiable in-  
 584 formation (PII) or sensitive content is present in  
 585 any of the datasets.

586 We use LLaMA-2 and LLaMA-3 models un-  
 587 der Meta’s official research license, and all model  
 588 adaptations are conducted in compliance with their  
 589 intended use for academic and non-commercial  
 590 research. The training and evaluation procedures  
 591 are entirely conducted on benchmark data, and no  
 592 human subjects are involved.

593 We adhere to the ethical guidelines set forth by  
 594 the ACL Code of Ethics, including transparency,  
 595 reproducibility, and the responsible use of language  
 596 models. Our work poses minimal risk of harm  
 597 and does not involve content generation, human  
 598 annotation, or interaction with real users.

## References

Elizabeth Boschee, Jennifer Lautenschlager, Sean O'Brien, Steve Shellman, James Starz, and Michael Ward. 2015. *ICEWS Coded Event Data*.

Rochana Chaturvedi. 2024. *Temporal knowledge graph extraction and modeling across multiple documents for health risk prediction*. In *Companion Proceedings of the ACM Web Conference 2024*, pages 1182–1185.

Kai Chen, Ye Wang, Yitong Li, and Aiping Li. 2022. Rotateqvs: Representing temporal information as rotations in quaternion vector space for temporal knowledge graph completion. *arXiv preprint arXiv:2203.07993*.

Ambedkar Dukkipati, Kawin Mayilvaghanan, Naveen Kumar Pallekonda, Sai Prakash Hadnoor, and Ranga Shaarad Ayyagari. 2025. *Predictive ai with external knowledge infusion for stocks*. *arXiv preprint arXiv:2504.20058*.

Julia Gastinger, Timo Sztyler, Lokesh Sharma, Anett Schuelke, and Heiner Stuckenschmidt. 2023. *Comparing apples and oranges? on the evaluation of methods for temporal knowledge graph forecasting*. In *Joint European Conference on Machine Learning and Knowledge Discovery in Databases*, pages 533–549. Springer.

Zhen Han, Peng Chen, Yunpu Ma, and Volker Tresp. 2020. *Explainable subgraph reasoning for forecasting on temporal knowledge graphs*. In *International Conference on Learning Representations*.

Zhen Han, Zifeng Ding, Yunpu Ma, Yujia Gu, and Volker Tresp. 2021. *Learning neural ordinary equations for forecasting future links on temporal knowledge graphs*. In *Proceedings of the 2021 Conference on Empirical Methods in Natural Language Processing*, pages 8352–8364.

Edward J. Hu, Yelong Shen, Phillip Wallis, Zeyuan Allen-Zhu, Yuanzhi Li, Shean Wang, Lu Wang, and Weizhu Chen. 2022. *Lora: Low-rank adaptation of large language models*. In *International Conference on Learning Representations (ICLR)*.

Yixin Ji, Juntao Li, Hai Ye, Kaixin Wu, Kai Yao, Jia Xu, Linjian Mo, and Min Zhang. 2025. *Test-time compute: from system-1 thinking to system-2 thinking*. *Preprint*, arXiv:2501.02497.

Woojeong Jin, Meng Qu, Xisen Jin, and Xiang Ren. 2020. *Recurrent event network: Autoregressive structure inference over temporal knowledge graphs*. In *Proceedings of the 2020 Conference on Empirical Methods in Natural Language Processing (EMNLP)*, pages 6669–6683.

Dong-Ho Lee, Kian Ahrabian, Woojeong Jin, Fred Morstatter, and Jay Pujara. 2023. *Temporal knowledge graph forecasting without knowledge using in-context learning*. *Preprint*, arXiv:2305.10613.

Kalev Leetaru and Philip A Schrod. 2013. Gdelt: Global data on events, location, and tone, 1979–2012. In *ISA annual convention*, volume 2, pages 1–49. Citeseer.

Aitor Lewkowycz, Anders Andreassen, David Dohan, Ethan Dyer, Henryk Michalewski, Vinay Ramasesh, Ambrose Slone, Cem Anil, Imanol Schlag, Theo Gutman-Solo, Yuhuai Wu, Behnam Neyshabur, Guy Gur-Ari, and Vedant Misra. 2022. *Solving quantitative reasoning problems with language models*. In *Proceedings of the 2022 Conference on Empirical Methods in Natural Language Processing*, Online. Association for Computational Linguistics.

Zixuan Li, Xiaolong Jin, Wei Li, Saiping Guan, Jiafeng Guo, Huawei Shen, Yuanzhuo Wang, and Xueqi Cheng. 2021. *Temporal knowledge graph reasoning based on evolutional representation learning*. In *Proceedings of the 44th International ACM SIGIR Conference on Research and Development in Information Retrieval*, pages 408–417.

Ruotong Liao, Xu Jia, Yangzhe Li, Yunpu Ma, and Volker Tresp. 2024. *Gentkg: Generative forecasting on temporal knowledge graph with large language models*. *Preprint*, arXiv:2310.07793.

Yushan Liu, Yunpu Ma, Marcel Hildebrandt, Mitchell Joblin, and Volker Tresp. 2022. *Tlogic: Temporal logical rules for explainable link forecasting on temporal knowledge graphs*. In *Proceedings of the Thirty-Sixth AAAI Conference on Artificial Intelligence (AAAI)*, pages 4120–4127.

Ruilin Luo, Tianle Gu, Haoling Li, Junzhe Li, Zicheng Lin, Jiayi Li, and Yujiu Yang. 2024. *Chain of history: Learning and forecasting with llms for temporal knowledge graph completion*. *Preprint*, arXiv:2401.06072.

Farzaneh Mahdisoltani, Joanna Biega, and Fabian M Suchanek. 2013. *Yago3: A knowledge base from multilingual wikipedias*. In *CIDR*.

Shreyas Mangrulkar and 1 others. 2022. Peft: parameter-efficient fine-tuning. <https://github.com/huggingface/peft>. GitHub repository, accessed May 2025.

Johannes Messner, Ralph Abboud, and Ismail Ilkan Ceylan. 2022. *Temporal knowledge graph completion using box embeddings*. In *Proceedings of the AAAI Conference on Artificial Intelligence*, volume 36, pages 7779–7787.

Meta AI. 2024. *Meta llama 3: Open foundation and fine-tuned chat models*. <https://ai.meta.com/blog/meta-llama-3/>. Accessed: 2025-05-16.

Michael Schlichtkrull, Thomas N Kipf, Peter Bloem, Rianne Van Den Berg, Ivan Titov, and Max Welling. 2018. *Modeling relational data with graph convolutional networks*. In *European semantic web conference*, pages 593–607. Springer.

708 Sentence-Transformers. all-mpnet-base-v2. <https://huggingface.co/sentence-transformers/all-mpnet-base-v2>. Accessed: 2025-05-19. 763  
709 764  
710 765  
711 766  
712 767  
713 768  
714

715 Charlie Snell, Jaehoon Lee, Kelvin Xu, and Aviral Kumar. 2024. Scaling llm test-time compute optimally 769  
716 can be more effective than scaling model parameters. 770  
717 *Preprint*, arXiv:2408.03314. 771

718 Kaitao Song, Xu Tan, Tao Qin, Jianfeng Lu, and Tie- 772  
719 Yan Liu. 2020. Mpnet: Masked and permuted pre- 773  
720 training for language understanding. In *Advances in 774  
721 Neural Information Processing Systems*, volume 33, 775  
722 pages 16857–16867. 776

723 Haohai Sun, Jialun Zhong, Yunpu Ma, Zhen Han, and 777  
724 Kun He. 2021. Timetraveler: Reinforcement learning 778  
725 for temporal knowledge graph forecasting. *arXiv 779  
726 preprint arXiv:2109.04101*. 780

727 Hugo Touvron, Louis Martin, Kevin Stone, Abdul- 781  
728 lah Al-Dujaili, Yasmine Babaei, Nikolay Bashlykov, 782  
729 Soumya Batra, Prajwal Bhargava, Shruti Bhosale, and 1 others. 2023. Llama 2: Open founda- 783  
730 tion and fine-tuned chat models. *arXiv preprint 784  
731 arXiv:2307.09288*. 785

732 Volker Tresp, Cristóbal Esteban, Yinchong Yang, 788  
733 Stephan Baier, and Denis Krompaß. 2015. Learning 789  
734 with memory embeddings. *arXiv preprint 790  
735 arXiv:1511.07972*. 791

736 Rakshit Trivedi, Hanjun Dai, Yichen Wang, and 792  
737 Le Song. 2017. Know-evolve: Deep temporal reason- 793  
738 ing for dynamic knowledge graphs. In *Proceedings 794  
739 of the 34th International Conference on Machine 795 Learning*, pages 3462–3471. PMLR. 796

740 Shangshang Wang, Julian Asilis, Ömer Faruk Akgül, 797  
741 Enes Burak Bilgin, Ollie Liu, and Willie Neiswanger. 798  
742 2025. Tina: Tiny reasoning models via lora. *arXiv 799  
743 preprint arXiv:2504.15777*. 800

744 Yuwei Xia, Ding Wang, Qiang Liu, Liang Wang, Shu 803  
745 Wu, and Xiao-Yu Zhang. 2024a. Chain-of-history 804  
746 reasoning for temporal knowledge graph forecasting. 805  
747 In *Findings of the Association for Computational 806  
748 Linguistics: ACL 2024*, pages 16144–16159, Bangkok, 807  
Thailand. Association for Computational Linguistics. 808

749 Yuwei Xia, Ding Wang, Qiang Liu, Liang Wang, Shu 809  
750 Wu, and Xiao-Yu Zhang. 2024b. Chain-of-history 810  
751 reasoning for temporal knowledge graph forecasting. 811  
752 In *Findings of the Association for Computational 813  
753 Linguistics: ACL 2024*. 814

754 Wenjie Xu, Ben Liu, Miao Peng, Xu Jia, and Min Peng. 815  
755 2023. Pre-trained language model with prompts 816  
756 for temporal knowledge graph completion. *arXiv 817  
757 preprint arXiv:2305.07912*. 818

758 Wenjie Xu, Ben Liu, Miao Peng, Zihao Jiang, Xu Jia, 819  
759 Kai Liu, Lei Liu, and Min Peng. 2025. Historical 820  
760 facts learning from long-short terms with language 821  
761 model for temporal knowledge graph reasoning. *In- 822  
762 formation Processing & Management*, 62(3):104047. 823

## 769 A Rule-Based Multi-Hop History 770 Sampling Details

### 771 A.1 TLR Algorithm

772 Algorithm 1 shows the TLR retrieval procedure  
773 used in our framework, reproduced from (Liao  
774 et al., 2024).

---

#### Algorithm 1 TLR Retrieval

---

**Input:** Temporal knowledge graph  $\mathcal{G}$ , query  $(s_q, r_q, ?, T)$ , learned rules  $\mathcal{TR}$

**Output:** A set of retrieved facts  $\mathcal{G}_{s_q}(s_q, r_q, T)$

```

1:  $\mathcal{G}_{s_q}(s_q, r_q, T) \leftarrow \emptyset$ 
2: for  $fact \leftarrow (s_q, r_q, o, t < T) \in \mathcal{G}$  do
3:    $\mathcal{G}_{s_q}(s_q, r_q, T) \leftarrow \mathcal{G}_{s_q}(s_q, r_q, T) \cup fact$ 
4: end for
5: for top k rules w.r.t.  $r_q \leftarrow r_b \in \mathcal{TR}$  do
6:   Get a list  $r_b \leftarrow \{r_{b_1}, r_{b_2}, \dots, r_{b_k}\}$ 
7: end for
8: for  $fact \leftarrow (s_q, r \in r_b, o, t < T) \in \mathcal{G}$  do
9:    $\mathcal{G}_{s_q}(s_q, r_q, T) \leftarrow \mathcal{G}_{s_q}(s_q, r_q, T) \cup fact$ 
10: end for
11: return  $\mathcal{G}_{s_q}(s_q, r_q, T)$ 

```

---

## 775 A.2 Context-guided Multi-hop Expansion 776 Details

### 777 A.2.1 Weight Formulation Discussion

778 We adopt a multiplicative combination of the  
779 weight components rather than a simple sum to  
780 for two reasons. First, the neighbor weight  $w_n$  acts  
781 as a hard constraint: it equals zero if the subject  
782 or object of a candidate quadruple is not reachable  
783 from the query, effectively filtering out irrelevant  
784 facts. Second, the frequency weight  $w_f$  is designed  
785 to down-weight commonly repeated triples while  
786 preserving their relative order. This logarithmic  
787 scaling ensures that rare but structurally relevant  
788 facts are not overshadowed. Together, the multi-  
789 plicative form enables a soft prioritization across  
790 dimensions while preserving hard structural con-  
791 straints.

### 792 A.2.2 Weight Component

793 The five weight components of equation 2 are de-  
794 fined as follows:

795 **Neighbor weight**  $w_n$  ensures that structurally  
796 closer quadruples receive higher scores:

$$797 w_n = \exp(-\gamma_1 \cdot (\text{hop}_s + \text{hop}_o - 1)),$$

798 where  $\text{hop}_s$  and  $\text{hop}_o$  denote the shortest hop dis-  
799 tances from the subject and object to the query

800 subject. The weight decays exponentially with in-  
801 creasing distance, and vanishes to zero when either  
802  $\text{hop}_s$  or  $\text{hop}_o$  is infinite, corresponding to cases  
803 where the entity is not reachable from the query  
804 subject in the graph. Importantly, all structural  
805 statistics (e.g., hop distance, co-occurrence counts,  
806 and context connectivity) are computed over the  
807 subgraph excluding quadruples with timestamps  
808 after the query time  $T$ .

809 **Frequency weight**  $w_f$  reduces the dominance  
810 of frequent triples (history quadruples excluding  
811 timestamp):

$$812 w_f = \frac{1}{\gamma_2 \cdot \log(n_{spo}) + 1},$$

813 where  $n_{spo}$  is the count of the subject-predicate-  
814 object triple. This logarithmic form discourages  
815 over-sampling of repetitive patterns while maintain-  
816 ing frequency order.

817 More precisely, for any two triples with fre-  
818 quency counts  $n_1 < n_2$ , the corresponding weights  
819 satisfy:

$$820 w(n_1) > w(n_2), \quad \text{and} \quad \frac{w(n_1)}{w(n_2)} = \frac{\log(n_2) + 1}{\log(n_1) + 1},$$

821 assuming all other components of the weight func-  
822 tion are equal. This shows that the multiplicative  
823 formulation preserves the relative ranking induced  
824 by frequency, while still suppressing the absolute  
825 dominance of highly frequent triples.

826 **Time weight**  $w_t$  favors temporally recent events:

$$827 w_t = \exp\left(-\gamma_3 \cdot \frac{T - t}{\delta}\right),$$

828 where  $T$  is the timestamp of the query,  $t$  is the  
829 timestamp of the event quadruple (with  $T > t$ ),  $\delta$   
830 is the time granularity (e.g.,  $\delta = 24$  in ICEWS14),  
831 and  $\gamma_3$  controls the decay rate.

832 **Connection weight**  $w_c$  promotes inclusion of  
833 frequently co-occurring entity pairs:

$$834 w_c = \frac{\log(1 + \gamma_4 \cdot n_{so})}{1 + \log(1 + \gamma_4 \cdot n_{so})},$$

835 where  $n_{so}$  is the co-occurrence count of the subject-  
836 object pair prior to  $T$ , and  $\gamma_4$  is a smoothing param-  
837 eter. This bounded function emphasizes structural  
838 relevance while limiting hub bias.

839 **Contextual priority weight**  $w_{cp}$  encourages  
840 sampling quadruples that remain connected to the  
841 initial TLR sampled subgraph:

$$842 w_{cp} = \begin{cases} 1, & \text{if } s \in \mathcal{E}_{\text{TLR}} \text{ or } o \in \mathcal{E}_{\text{TLR}}, \\ 0, & \text{otherwise,} \end{cases}$$

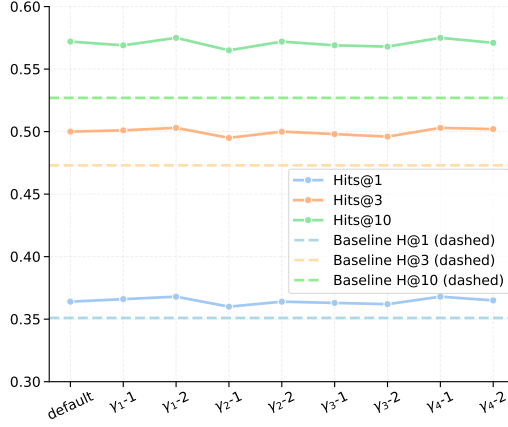


Figure 6: Performance of ICL-RBMH under different sampling hyperparameter configurations.

where  $\mathcal{E}_{\text{TLR}}$  is the set of all 1-hop neighbors identified in the TLR stage. This guides the expansion toward semantically coherent subgraphs.

### A.2.3 Hyperparameter Sensitivity Experiment

Figure 6 presents the performance in ICL-RBMH setting under varying sampling hyperparameters. We perturb each of the four  $\gamma_i$  parameters individually (two settings per parameter), while keeping others fixed, and compare them against the default configuration. Across all variants, model performance remains stable, indicating that *RBMH Sampling* is robust to hyperparameter choices. Moreover, ICL-RBMH consistently outperforms the baseline ICL-TLR across all settings.

The sampling hyperparameter configurations and their corresponding performance metrics are summarized in Table 6, including mean and standard deviation to reflect stability.

Table 6: Performance of ICL-RBMH under different sampling hyperparameter configurations on ICEWS14.

ID	$\gamma_1$	$\gamma_2$	$\gamma_3$	$\gamma_4$	Hits@1	Hits@3	Hits@10		
default	0.6	0.6	0.01	0.1	0.364	0.500	0.572		
$\gamma_1^{-1}$	0.4	0.6	0.01	0.1	0.366	0.501	0.569		
$\gamma_1^{-2}$	0.8	0.6	0.01	0.1	0.368	0.504	0.575		
$\gamma_2^{-1}$	0.6	0.4	0.01	0.1	0.364	0.500	0.572		
$\gamma_2^{-2}$	0.6	0.8	0.01	0.1	0.364	0.500	0.572		
$\gamma_3^{-1}$	0.6	0.6	0.05	0.1	0.363	0.498	0.569		
$\gamma_3^{-2}$	0.6	0.6	0.002	0.1	0.368	0.506	0.573		
$\gamma_4^{-1}$	0.6	0.6	0.01	0.2	0.368	0.503	0.575		
$\gamma_4^{-2}$	0.6	0.6	0.01	0.05	0.365	0.502	0.571		
Mean		0.366		0.501		0.571			
Std		0.0020		0.0024		0.0021			
Baseline (ICL-TLR)				0.351		0.473			
				0.527					

### A.3 RBMH Algorithm

#### Algorithm 2 Rule-based Multi-hop history sampling

**Input:** Temporal knowledge graph  $\mathcal{G}$ , query  $(s_q, r_q, ?, T)$ , learned rules  $\mathcal{TR}$ , maximum history length  $N$ , scoring function  $\mathcal{F}$ , a set of TLR retrieved facts  $\mathcal{G}_{s_q}(s_q, r_q, T)$

**Output:** A set of retrieved facts  $\mathcal{G}(s_q, r_q, T)$

```

1:  $M \leftarrow N - \text{len}(\mathcal{G}_{s_q}(s_q, r_q, T))$ 
2: if  $M = 0$  then
3:    $\mathcal{G}(s_q, r_q, T) \leftarrow \mathcal{G}_{s_q}(s_q, r_q, T)$ 
4:   return  $\mathcal{G}(s_q, r_q, T)$ 
5: end if
6:  $\mathcal{C} \leftarrow \{(s, r, o, t, \mathcal{F}(s, r, o, t)) \mid (s, r, o, t) \in \mathcal{G}, t < T\}$ 
7:  $\mathcal{C}_{\text{top}} \leftarrow \text{Top}_{10M}(\mathcal{C})$ 
8:  $\mathcal{C}_{\text{sample}} \leftarrow \text{WeightedSample}(\mathcal{C}_{\text{top}}, M)$ 
9:  $\mathcal{G}_{\text{mh}}(s_q, r_q, T) \leftarrow \{(s, r, o, t) \mid (s, r, o, t, w) \in \mathcal{C}_{\text{sample}}\}$ 
10:  $\mathcal{G}(s_q, r_q, T) \leftarrow \mathcal{G}_{s_q}(s_q, r_q, T) \cup \mathcal{G}_{\text{mh}}(s_q, r_q, T)$ 
11: return  $\mathcal{G}(s_q, r_q, T)$ 

```

### B Computational Efficiency Analysis

RECIPE-TKG is designed to be parameter-efficient and computationally lightweight while maintaining strong performance. This section quantifies various aspects of efficiency in our framework.

**Parameter Efficiency** Our framework fine-tunes a small fraction of the total parameters in the base LLM. For LLaMA2-7B, we update only LoRA adapters (with rank 8, applied to query and value projections across 32 transformer layers) and a self-attention pooling module for entity embedding aggregation. The trainable parameter count is approximately 54.3M, which constitutes just 0.81% of the base model’s 6.74B parameters. This parameter-efficient design enables effective fine-tuning while keeping most of the pre-trained knowledge intact.

**Rule Mining Efficiency** The temporal logical rule mining process in our RBMH sampling strategy is highly efficient. Table 7 shows the time required for rule extraction across all datasets using 15 CPU processes (averaged over 5 runs). The process completes in under 20 seconds even for the largest dataset, representing negligible computational overhead. Furthermore, the extracted rules capture persistent temporal patterns and are not highly sensitive to minor dataset changes, allowing

889 for infrequent updates when the knowledge graph  
 890 evolves.

Table 7: Rule mining time across datasets (in seconds).

Dataset	ICEWS14	ICEWS18	GDELT	YAGO
Time (s)	$6.89 \pm 0.08$	$16.72 \pm 0.07$	$10.78 \pm 0.08$	$2.73 \pm 0.02$

891 **Training Overhead** Table 8 compares training  
 892 time per epoch between standard supervised  
 893 fine-tuning and our contrastive fine-tuning on 1024  
 894 samples. The contrastive objective introduces no  
 895 additional training time, demonstrating its compu-  
 896 tational efficiency despite the improved semantic  
 897 learning.

Table 8: Training time per epoch on 1024 samples.

Training Mode	Time (s)	$\Delta\%$
Fine-tuning (FT)	824.31	-
FT + Contrastive Loss	821.51	-0.34%

898 **Inference Overhead** Table 9 quantifies the  
 899 run-time impact of our test-time filtering mechanism.  
 900 On 1,000 test samples, filtering increases inference  
 901 time by 16.6%, which is reasonable considering the  
 902 consistent performance improvements in Hits@10  
 903 across all datasets. The filtering step provides a  
 904 favorable trade-off between computational cost and  
 905 accuracy gain.

Table 9: Inference time on 1,000 samples.

Setting	Time (s)	$\Delta\%$
No filtering	2316.48	-
With filtering	2700.67	+16.60%

## C Training Details

### C.1 Relation Classification

908 The prompt used for relation classification is pro-  
 909 vided in Figure 7.

910 In cases where a neighbor is connected to the  
 911 anchor via both a positive and a negative relation,  
 912 it is excluded in training to avoid ambiguity.

913 Figure 8 shows the distribution of relation types  
 914 across four datasets. Positive and negative relations  
 915 appear in roughly balanced proportions, while neu-  
 916 tral relations are consistently less common. Nota-  
 917 bly, YAGO exhibits a distinct relation distribu-  
 918 tion where the majority of relations are classified as  
 919 *neutral*. Upon inspection, we find that this reflects

920 the actual semantic nature of the relations in the  
 921 dataset, which are mostly descriptive or taxonomic  
 922 rather than sentiment-oriented. Consequently, the  
 923 contrastive learning component has limited impact  
 924 on YAGO, as it relies on meaningful distinctions be-  
 925 tween positive and negative relations. The observed  
 926 performance gain on YAGO is therefore primarily  
 927 attributed to improvements in history sampling and  
 928 *Test-time filtering*.

### C.2 Prompt

929 To guide the language model in performing tempo-  
 930 ral knowledge completion, we adopt a structured,  
 931 instruction-style prompt format shown in Figure 9.  
 932 The prompt defines the task explicitly: given a  
 933 chronological list of historical events represented  
 934 as quadruples, the model must predict the missing  
 935 object entity for a future temporal query.

936 Each historical fact is formatted  
 937 as `{time}:{[subject}, {relation},`  
 938 `{object_label}.{object}]` where  
 939 `{object_label}` is a unique identi-  
 940 fier associated with the entity (e.g.,  
 941 3380.Joseph\_Robinette\_Biden). This la-  
 942 beling scheme facilitates consistent reference  
 943 resolution and improves post-processing via  
 944 regex-based extraction. The final input ends  
 945 with the query, and the model is asked to gen-  
 946 erate the correct object in fully qualified form  
 947 `{object_label}.{object}`.

948 This prompt format is applied consistently across  
 949 both in-context learning and fine-tuning setups.

### C.3 LoRA Formulation

950 We follow the standard LoRA setup (Hu et al.,  
 951 2022). Given a frozen pretrained weight matrix  
 952  $W_0 \in \mathbb{R}^{d \times k}$ , LoRA introduces two trainable low-  
 953 rank matrices  $A \in \mathbb{R}^{d \times r}$  and  $B \in \mathbb{R}^{r \times k}$  with  
 954  $r \ll \min(d, k)$ , such that the original forward  
 955 transformation  $h(x) = W_0x$  is modified as:

$$\hat{h}(x) = W_0x + ABx. \quad (10)$$

956 This design allows efficient fine-tuning by only  
 957 training  $A$  and  $B$ , while keeping the pretrained  
 958 weights  $W_0$  frozen. In our experiments, we adopt  
 959 the default LoRA implementation from the PEFT  
 960 library (Mangrulkar et al., 2022).

### C.4 Implementation Details

964 We fine-tune LLaMA-2-7B and LLaMA-3-8B models  
 965 using LoRA adapters. All trainings are conducted

## Prompt for Relation Classification

You are analyzing relation labels from a political event knowledge graph, where each relation reflects an action or request within a geopolitical context.

Classify the sentiment of the given relation as one of the following:

- **positive** (e.g., promoting peace, aid, cooperation)
- **negative** (e.g., violence, repression, aggression)
- **neutral** (e.g., procedural or ambiguous actions)

Avoid selecting "neutral" unless the relation is genuinely ambiguous or purely procedural in nature.

Figure 7: Prompt used for relation classification.

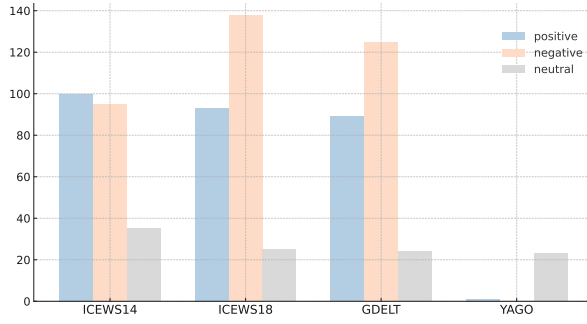


Figure 8: Distribution of relation types in four datasets after automatic classification.

Table 10: Performance under different contrastive weight settings on ICEWS14.

Weight $\alpha$	Hits@1	Hits@3	Hits@10
0.2	0.392	0.521	0.580
0.5	0.389	0.521	0.579
0.8	0.392	0.520	0.576
Mean	0.391	0.521	0.578
Std	0.0014	0.0006	0.0020

is robust to the choice of  $\alpha$ , and that *CFT* contributes consistently across a wide range of weighting schemes. Table 10 presents the sensitivity of model performance to the contrastive weight  $\alpha$ . The consistently small standard deviations across metrics suggest that the model is robust to variations in  $\alpha$ .

## D Test-Time Filtering

**Embedding Model.** To compute semantic similarity between predictions and context, we use the `all-mpnet-base-v2` model (Song et al., 2020; Sentence-Transformers) from HuggingFace, a pre-trained sentence transformer with 768-dimensional output. We treat both the generated prediction string and the full in-context prompt as input sequences and extract mean-pooled embeddings for similarity calculation.

**Similarity Distribution Analysis.** We analyze the cosine similarity  $\phi(p, c)$  between prediction and context across 7,371 test samples from ICEWS14 using the contrastively tuned model. The average similarity score for correct predictions exceeds that of incorrect ones by  $\Delta\mu = 0.057$ . This supports

967 on 2 H100 GPUs in bfloat16 precision. We set  
968 maximum history length to 50 in history sampling  
969 according to the context length of LLaMA-2-7B. For  
970 fine-tuning, we train 1024-shots data for 50 epochs  
971 with the batch size of 512, the learning rate of 3e-4,  
972 the context length of 4096, the target length of 128,  
973 the LoRA rank of 8, the LoRA dropout rate of 0.05.  
974 For RECIPE-TKG, we train 6024-shots data (1024  
975 aligned with GenTKG and 5000 randomly sampled  
976 by seed 42) for 10 epochs, and other settings keep  
977 unchanged. Contrastive tuning uses a margin of 1.0  
978 and loss weight  $\alpha = 0.2$  to balance cross-entropy  
979 and contrastive objectives.

980 Entities are tokenized using the native tokenizer  
981 of the LLM and embedded via the model’s em-  
982 bedding layer. A lightweight attention aggregator  
983 produces final entity embeddings, jointly trained  
984 with the model.

## C.5 Hyperparameter Sensitivity Experiment

985 As shown in Figure 10, varying  $\alpha$  from 0.2 to 0.8  
986 leads to marginal fluctuations across all evalua-  
987 tion metrics. These results suggest that the model  
988

989  
990  
991  
992  
993  
994  
995

996  
997  
998  
999  
1000  
1001  
1002  
1003  
1004  
1005

1006  
1007  
1008  
1009  
1010  
1011

## Prompt Example

You must be able to correctly predict the next {object} from a given text consisting of multiple quadruplets in the form of "{time}:[{subject}, {relation}, {object\_label}.{object}]" and the query in the form of "{time}:[{subject}, {relation},]" in the end. You must generate {object\_label}.{object}.

2014-01-15: [Mehmet\_Simsek, Make\_statement, 5195.Other\_Authorities\_(Turkey)]  
 2014-01-20: [Nuri\_al-Maliki, Consult, 3380.Joseph\_Robinette\_Biden]  
 2014-01-25: [Joseph\_Robinette\_Biden, Make\_an\_appeal, 3990.Massoud\_Barzani]  
 2014-02-01: [Joseph\_Robinette\_Biden, Make\_an\_appeal\_or\_request,

Figure 9: Instruction-style prompt format for TKG forecasting.

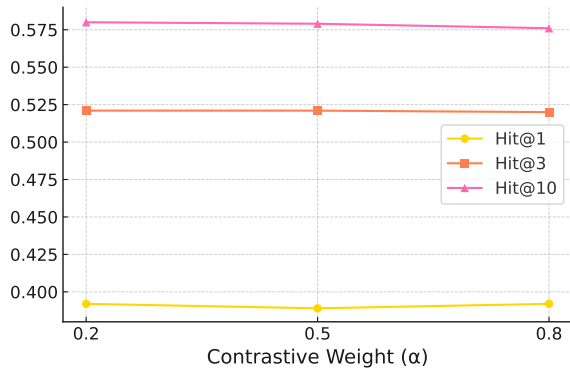


Figure 10: Effect of contrastive weight ( $\alpha$ )

our assumption that similarity can serve as a proxy for semantic plausibility.

**Novelty vs. Utility.** We further observe that:

- 9.1% of predictions are non-historical despite the gold answer being present in  $\mathcal{H}$ .
- Among all non-historical predictions, only 1.5% are correct and improve Hits@10.

These findings indicate that many model generations deviate from the historical context unnecessarily and fail to yield substantial gains. They motivate fallback to more salient entities when regeneration fails.

**Threshold Optimization.** The optimal threshold  $\tau^*$  is learned by maximizing separation between correct ( $\mathcal{C}$ ) and incorrect ( $\mathcal{I}$ ) prediction similarities:

$$\tau^* = \arg \max_{\tau} [F_{\mathcal{C}}(\tau) - F_{\mathcal{I}}(\tau)] \quad (11)$$

where  $F$  is the empirical CDF of cosine similarity values over samples from  $\mathcal{C}$  and  $\mathcal{I}$ .

**Fallback Scoring.** If generation fails after  $k$  iterations (we use  $k = 1$ ), the model selects a final answer from  $\mathcal{H}$  using:

$$f(h) = \frac{\text{count}(h)}{|\mathcal{H}|}, \quad (12)$$

$$r(h) = 1 - \frac{\text{pos}(h)}{|\mathcal{H}|}, \quad (13)$$

$$\psi(h) = \beta \cdot f(h) + (1 - \beta) \cdot r(h), \quad (14)$$

where  $\text{pos}(h)$  denotes the rank of  $h$  in its occurrence order. We set  $\beta = 0.6$  in all experiments.

We compute cosine similarities between predicted entities and prompt context using the all-mpnet-base-v2 sentence transformer from HuggingFace. The threshold  $\tau^*$  is tuned on a development set by maximizing the separation between correct and incorrect predictions.

Figure 11 examines the effect of the semantic filtering threshold  $\tau$ . As the threshold increases, Hits@10 improves, peaking near  $\tau = 0.6$ . Always falling back to historical entities ( $\tau = 1.0$ ) slightly increases accuracy at the cost of exploration and computational efficiency. Threshold  $\tau = 0.6$  balances correction with flexibility, enabling the model to revise low-quality outputs without overconstraining its generation space.

## E Cross-Dataset Filtering Performance

To evaluate the robustness and generalization capability of our test-time filtering approach, we analyze its performance across all four benchmark datasets. While the filtering mechanism was introduced primarily to reduce hallucinations in open-ended generation, an important question is whether this component generalizes well across different temporal knowledge domains or if its effectiveness is dataset-dependent.

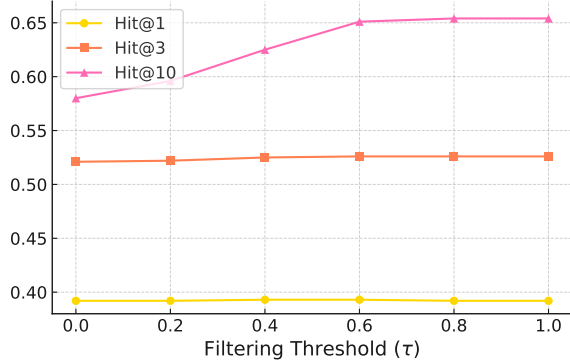


Figure 11: Effect of filtering threshold ( $\tau$ )

Table 11: Effect of filtering across datasets.

Method	Hits@1	Hits@3	Hits@10
<i>ICEWS14</i>			
RECIPE-TKG	0.393	0.526	0.651
RECIPE-TKG w/o Filter	0.392	0.521	0.580
<i>ICEWS18</i>			
RECIPE-TKG	0.224	0.369	0.516
RECIPE-TKG w/o Filter	0.242	0.382	0.437
<i>GDELT</i>			
RECIPE-TKG	0.095	0.192	0.327
RECIPE-TKG w/o Filter	0.092	0.189	0.266
<i>YAGO</i>			
RECIPE-TKG	0.811	0.880	0.930
RECIPE-TKG w/o Filter	0.759	0.822	0.842

Table 11 shows the impact of our similarity-based filtering module across all datasets by comparing the full RECIPE-TKG framework against a variant without filtering. The filtering module consistently improves Hits@10 across all datasets, with gains ranging from 7.1 percentage points (ICEWS14) to 9.4 percentage points (GDELT). Most notably, on the YAGO dataset, the filtering mechanism substantially improves performance across all metrics (Hits@1/3/10), suggesting particular effectiveness on datasets with more descriptive entities and varied relation types.

These results demonstrate that the filtering mechanism’s effectiveness is not dependent on dataset-specific properties, but rather reflects a general principle: by enforcing semantic consistency between predictions and input context, we can enhance model performance across diverse temporal knowledge domains. The observed consistency suggests that contextual alignment serves as a reliable signal for identifying and correcting implausible outputs, regardless of the specific entities and relations involved.

## F Baseline Model Details

We compare RECIPE-TKG against several baseline methods that reflect the dominant modeling paradigms for TKG forecasting. Embedding-based methods include RE-GCN (Li et al., 2021), which applies relational graph convolutions to timestamped graph snapshots; xERTE (Han et al., 2020), which combines subgraph sampling and path-based reasoning using attention for explainability; TANGO (Han et al., 2021), which uses neural ODEs to learn continuous-time entity embeddings; and TimeTraveler (Sun et al., 2021), which employs reinforcement learning to explore multi-hop temporal paths. Rule-based method includes TLogic (Liu et al., 2022) relies on extracted symbolic rules for forecasting. The results of these models are derived from Liao et al. (2024)

We also replicate two recent LLM-based methods. ICL (Lee et al., 2023) applies in-context learning by prepending historical quadruples to a query and using greedy decoding with a regex-based answer extraction. GenTKG (Liao et al., 2024) performs parameter-efficient fine-tuning with LoRA adapters, and combines this with a rule-based history sampling module. We use their official codebases and replicate their evaluation pipelines for fair comparison.

## G Baseline Model Details

We compare RECIPE-TKG against several baseline methods that reflect the dominant modeling paradigms for TKG forecasting.

**Embedding-based methods** include RE-GCN (Li et al., 2021), which applies relational graph convolutions to timestamped graph snapshots; RE-NET (Jin et al., 2020), which applies R-GCN (Schlichtkrull et al., 2018) for message passing for each snapshot and then uses temporal aggregation across multiple snapshots; xERTE (Han et al., 2020), which combines subgraph sampling and path-based reasoning using attention for explainability; TANGO (Han et al., 2021), which uses neural ODEs to learn continuous-time entity embeddings; and TimeTraveler (Sun et al., 2021), which employs reinforcement learning to explore multi-hop temporal paths.

**Rule-based method** TLogic (Liu et al., 2022) relies on extracted symbolic rules for forecasting.

1134 **LLM-based methods** We implement several re-  
1135 cent LLM-based approaches. ICL (Lee et al., 2023)  
1136 applies in-context learning by prepending histor-  
1137 ical quadruples to a query and using greedy de-  
1138 coding with regex-based answer extraction. Gen-  
1139 TKG (Liao et al., 2024) performs parameter-  
1140 efficient fine-tuning with LoRA adapters, com-  
1141 bined with rule-based history sampling. PPT (Xu  
1142 et al., 2023) converts quadruples into natural lan-  
1143 guage prompts and uses masked token prediction  
1144 to leverage semantic information from pretrained  
1145 language models. CoH (Xia et al., 2024b) ex-  
1146 plores high-order histories step-by-step to better  
1147 utilize richer historical information for LLM rea-  
1148 soning. HFL (Xu et al., 2025) learns from histor-  
1149 ical facts across different time periods through a  
1150 multi-perspective sampling strategy that focuses  
1151 on mining relational associations. We use official  
1152 codebases where available and replicate evaluation  
1153 pipelines for fair comparison.

1154 **Note on embedding-based baselines** Several  
1155 specialized embedding models for TKG com-  
1156 pletion (e.g., RotateQVS (Chen et al., 2022),  
1157 BoxTE (Messner et al., 2022), CGE (Ying et al.,  
1158 2024)) have shown strong performance but are  
1159 excluded from our main evaluation for three rea-  
1160 sons. First, they use different dataset splits (e.g.,  
1161 ICEWS14 with 72,826/8,941/8,963 train/valid/test  
1162 samples vs. our 74,845/8,514/7,371 split). Second,  
1163 embedding methods require task-specific mathe-  
1164 matical engineering, limiting cross-dataset gen-  
1165 eralizability, while LLM-based approaches ben-  
1166 efit from pre-trained knowledge and adaptability.  
1167 Third, there has been limited direct comparison be-  
1168 tween these paradigms in the literature. We include  
1169 only embedding-based methods using consistent  
1170 dataset splits for meaningful comparison.

## 1171 **H Dataset Statistics**

1172 We use four standard temporal knowledge graph  
1173 benchmarks. ICEWS14 and ICEWS18 are subsets  
1174 of the Integrated Crisis Early Warning System, con-  
1175 taining geopolitical event records with daily gran-  
1176 ularity. GDELT provides global political event data,  
1177 filtered to the most frequent events for tractability.  
1178 YAGO consists of curated facts from a multi-year  
1179 period. The statistics for these datasets are pro-  
1180 vided in Table 12.

## 1181 **I More Analysis**

### 1182 **I.1 Analysis of Contrastive Fine-Tuning**

1183 To complement the ablation results in Section 6.1,  
1184 we analyze how contrastive fine-tuning affects  
1185 model behavior in low-history regimes—settings  
1186 where standard exact-match metrics such as  
1187 Hits@k may fail to capture the semantic relevance  
1188 of model predictions.

1189 **Setup.** We group ICEWS14 test samples by his-  
1190 tory length and compute the semantic distance be-  
1191 tween each model prediction and the gold entity.  
1192 We compare three supervision settings: ICL, SFT,  
1193 and contrastive FT, all evaluated under the same  
1194 TLR history sampling.

1195 We define semantic distance using cosine simi-  
1196 larity between predicted and gold entities in a sen-  
1197 tence embedding space:

$$\phi(p, o) = 1 - \text{cos-sim}(E(p), E(o)), \quad (15)$$

1198 where  $E(\cdot)$  denotes the sentence transformer used  
1199 in Section 4.3. Lower  $\phi$  indicates higher semantic  
1200 alignment, even if the prediction does not exactly  
1201 match the gold entity.

1202 **Contrastive Tuning Improves Semantic Ground-  
1203 ing.** Figure 12 plots the semantic distance  $\phi(p, o)$   
1204 against the retrieved history length. All models  
1205 show the expected trend: greater history generally  
1206 yields predictions closer to the gold entity in em-  
1207 bedding space. However, the distinction between  
1208 supervision strategies becomes clear in low-history  
1209 regimes. In the encircled region (history length  
1210  $\leq 3$ ), contrastive fine-tuning produces fewer high-  
1211 distance predictions than both ICL and SFT. This  
1212 demonstrates that contrastive learning enhances the  
1213 model’s ability to infer plausible entities even when  
1214 the input lacks strong historical evidence.

### 1215 **Multi-hop Sampling Further Stabilizes Model**

1216 **Behavior.** To examine how our sampling strategy  
1217 affects model reasoning on sparse-history inputs,  
1218 we repeat the same experiment using our proposed  
1219 *RBMH Sampling*. For comparability, we compute  
1220 semantic distances on the same subset of samples  
1221 originally identified as short-history under TLR.

1222 As shown in Figure 13, contrastive-tuned mod-  
1223 els under *RBMH Sampling* exhibit more uniform  
1224 semantic behavior across history lengths. Unlike  
1225 the steep drop-off observed under TLR, the seman-  
1226 tic distance remains relatively stable, indicating  
1227 that many samples previously limited by shallow

Table 12: Dataset statistics used in our experiments. Time granularity varies by dataset and influences temporal resolution.

Dataset	#Train	#Valid	#Test	#Entities	#Relations	Time Gap
ICEWS14	74,845	8,514	7,371	7,128	230	1 day
ICEWS18	373,018	45,995	49,545	23,033	256	1 day
GDELT	79,319	9,957	9,715	5,850	238	15 mins
YAGO	220,393	28,948	22,765	10,778	24	1 year

1229 context can now be grounded through richer structural and temporal cues. This supports our motivation in Section 2.1: one-hop sampling often fails  
1230 to provide the necessary relational evidence, and  
1231 multi-hop expansion is essential for enabling reliable  
1232 reasoning, rather than the test instances being  
1233 inherently harder.  
1234

1235  
1236 **Qualitative Support.** Figure 14 presents qualitative examples where contrastive-tuned models  
1237 produce predictions that are not exact matches but  
1238 remain relationally and contextually appropriate. In  
1239 contrast, ICL and SFT often produce surface-level  
1240 or unrelated completions. These examples, paired  
1241 with the distributional evidence above, underscore  
1242 how contrastive fine-tuning improves semantic generalization and interpretability, particularly when  
1243 Hits@k offers limited signal.  
1244

1245  
1246 **Case Study.** To better understand the behavior  
1247 of RECIPE-TKG, we provide a case study  
1248 comparing the top-10 predictions of four methods  
1249 on a specific query. The ground-truth object is  
1250 `High_Ranking_Military_Personnel_(Nigeria)`,  
1251 which is not explicitly present in the history. As  
1252 shown in Figure 15, none of the models are  
1253 able to perfectly predict the correct entity.  
1254 However, the predictions made by RECIPE-  
1255 TKG models are clearly more semantically  
1256 aligned with the ground truth. For example,  
1257 predictions such as `Military_(Nigeria)` and  
1258 `Defense_Personnel_(Nigeria)` closely ap-  
1259 proximate the true answer in meaning, whereas  
1260 other models (ICL and GenTKG) fail to capture  
1261 such relevant semantics. This demonstrates the  
1262 advantage of contrastive fine-tuning in shaping the  
1263 embedding space, allowing the model to produce  
1264 more relationally compatible predictions even  
1265 when exact matches are not observed in history.  
1266

## J Use of AI Tools

1267 AI assistants were used to support writing (e.g.,  
1268 phrasing suggestions) and code generation (e.g.,  
1269 syntax templates). All such outputs were subject  
1270 to thorough human verification, and the authors  
1271 remain fully responsible for the content presented.  
1272

1273  
1274  
1275  
1276  
1277  
1278  
1279  
1280  
1281  
1282  
1283  
1284  
1285  
1286  
1287  
1288  
1289  
1290  
1291  
1292  
1293  
1294  
1295  
1296  
1297  
1298  
1299  
1300  
1301  
1302  
1303  
1304  
1305  
1306  
1307  
1308  
1309  
1310  
1311  
1312  
1313  
1314  
1315  
1316  
1317  
1318  
1319  
1320  
1321  
1322  
1323  
1324  
1325  
1326  
1327  
1328  
1329  
1330  
1331  
1332  
1333  
1334  
1335  
1336  
1337  
1338  
1339  
1340  
1341  
1342  
1343  
1344  
1345  
1346  
1347  
1348  
1349  
1350  
1351  
1352  
1353  
1354  
1355  
1356  
1357  
1358  
1359  
1360  
1361  
1362  
1363  
1364  
1365  
1366  
1367  
1368  
1369  
1370  
1371  
1372  
1373  
1374  
1375  
1376  
1377  
1378  
1379  
1380  
1381  
1382  
1383  
1384  
1385  
1386  
1387  
1388  
1389  
1390  
1391  
1392  
1393  
1394  
1395  
1396  
1397  
1398  
1399  
1400  
1401  
1402  
1403  
1404  
1405  
1406  
1407  
1408  
1409  
1410  
1411  
1412  
1413  
1414  
1415  
1416  
1417  
1418  
1419  
1420  
1421  
1422  
1423  
1424  
1425  
1426  
1427  
1428  
1429  
1430  
1431  
1432  
1433  
1434  
1435  
1436  
1437  
1438  
1439  
1440  
1441  
1442  
1443  
1444  
1445  
1446  
1447  
1448  
1449  
1450  
1451  
1452  
1453  
1454  
1455  
1456  
1457  
1458  
1459  
1460  
1461  
1462  
1463  
1464  
1465  
1466  
1467  
1468  
1469  
1470  
1471  
1472  
1473  
1474  
1475  
1476  
1477  
1478  
1479  
1480  
1481  
1482  
1483  
1484  
1485  
1486  
1487  
1488  
1489  
1490  
1491  
1492  
1493  
1494  
1495  
1496  
1497  
1498  
1499  
1500  
1501  
1502  
1503  
1504  
1505  
1506  
1507  
1508  
1509  
1510  
1511  
1512  
1513  
1514  
1515  
1516  
1517  
1518  
1519  
1520  
1521  
1522  
1523  
1524  
1525  
1526  
1527  
1528  
1529  
1530  
1531  
1532  
1533  
1534  
1535  
1536  
1537  
1538  
1539  
1540  
1541  
1542  
1543  
1544  
1545  
1546  
1547  
1548  
1549  
1550  
1551  
1552  
1553  
1554  
1555  
1556  
1557  
1558  
1559  
1560  
1561  
1562  
1563  
1564  
1565  
1566  
1567  
1568  
1569  
1570  
1571  
1572  
1573  
1574  
1575  
1576  
1577  
1578  
1579  
1580  
1581  
1582  
1583  
1584  
1585  
1586  
1587  
1588  
1589  
1590  
1591  
1592  
1593  
1594  
1595  
1596  
1597  
1598  
1599  
1600  
1601  
1602  
1603  
1604  
1605  
1606  
1607  
1608  
1609  
1610  
1611  
1612  
1613  
1614  
1615  
1616  
1617  
1618  
1619  
1620  
1621  
1622  
1623  
1624  
1625  
1626  
1627  
1628  
1629  
1630  
1631  
1632  
1633  
1634  
1635  
1636  
1637  
1638  
1639  
1640  
1641  
1642  
1643  
1644  
1645  
1646  
1647  
1648  
1649  
1650  
1651  
1652  
1653  
1654  
1655  
1656  
1657  
1658  
1659  
1660  
1661  
1662  
1663  
1664  
1665  
1666  
1667  
1668  
1669  
1670  
1671  
1672  
1673  
1674  
1675  
1676  
1677  
1678  
1679  
1680  
1681  
1682  
1683  
1684  
1685  
1686  
1687  
1688  
1689  
1690  
1691  
1692  
1693  
1694  
1695  
1696  
1697  
1698  
1699  
1700  
1701  
1702  
1703  
1704  
1705  
1706  
1707  
1708  
1709  
1710  
1711  
1712  
1713  
1714  
1715  
1716  
1717  
1718  
1719  
1720  
1721  
1722  
1723  
1724  
1725  
1726  
1727  
1728  
1729  
1730  
1731  
1732  
1733  
1734  
1735  
1736  
1737  
1738  
1739  
1740  
1741  
1742  
1743  
1744  
1745  
1746  
1747  
1748  
1749  
1750  
1751  
1752  
1753  
1754  
1755  
1756  
1757  
1758  
1759  
1760  
1761  
1762  
1763  
1764  
1765  
1766  
1767  
1768  
1769  
1770  
1771  
1772  
1773  
1774  
1775  
1776  
1777  
1778  
1779  
1780  
1781  
1782  
1783  
1784  
1785  
1786  
1787  
1788  
1789  
1790  
1791  
1792  
1793  
1794  
1795  
1796  
1797  
1798  
1799  
1800  
1801  
1802  
1803  
1804  
1805  
1806  
1807  
1808  
1809  
1810  
1811  
1812  
1813  
1814  
1815  
1816  
1817  
1818  
1819  
1820  
1821  
1822  
1823  
1824  
1825  
1826  
1827  
1828  
1829  
1830  
1831  
1832  
1833  
1834  
1835  
1836  
1837  
1838  
1839  
1840  
1841  
1842  
1843  
1844  
1845  
1846  
1847  
1848  
1849  
1850  
1851  
1852  
1853  
1854  
1855  
1856  
1857  
1858  
1859  
1860  
1861  
1862  
1863  
1864  
1865  
1866  
1867  
1868  
1869  
1870  
1871  
1872  
1873  
1874  
1875  
1876  
1877  
1878  
1879  
1880  
1881  
1882  
1883  
1884  
1885  
1886  
1887  
1888  
1889  
1890  
1891  
1892  
1893  
1894  
1895  
1896  
1897  
1898  
1899  
1900  
1901  
1902  
1903  
1904  
1905  
1906  
1907  
1908  
1909  
1910  
1911  
1912  
1913  
1914  
1915  
1916  
1917  
1918  
1919  
1920  
1921  
1922  
1923  
1924  
1925  
1926  
1927  
1928  
1929  
1930  
1931  
1932  
1933  
1934  
1935  
1936  
1937  
1938  
1939  
1940  
1941  
1942  
1943  
1944  
1945  
1946  
1947  
1948  
1949  
1950  
1951  
1952  
1953  
1954  
1955  
1956  
1957  
1958  
1959  
1960  
1961  
1962  
1963  
1964  
1965  
1966  
1967  
1968  
1969  
1970  
1971  
1972  
1973  
1974  
1975  
1976  
1977  
1978  
1979  
1980  
1981  
1982  
1983  
1984  
1985  
1986  
1987  
1988  
1989  
1990  
1991  
1992  
1993  
1994  
1995  
1996  
1997  
1998  
1999  
2000  
2001  
2002  
2003  
2004  
2005  
2006  
2007  
2008  
2009  
2010  
2011  
2012  
2013  
2014  
2015  
2016  
2017  
2018  
2019  
2020  
2021  
2022  
2023  
2024  
2025  
2026  
2027  
2028  
2029  
2030  
2031  
2032  
2033  
2034  
2035  
2036  
2037  
2038  
2039  
2040  
2041  
2042  
2043  
2044  
2045  
2046  
2047  
2048  
2049  
2050  
2051  
2052  
2053  
2054  
2055  
2056  
2057  
2058  
2059  
2060  
2061  
2062  
2063  
2064  
2065  
2066  
2067  
2068  
2069  
2070  
2071  
2072  
2073  
2074  
2075  
2076  
2077  
2078  
2079  
2080  
2081  
2082  
2083  
2084  
2085  
2086  
2087  
2088  
2089  
2090  
2091  
2092  
2093  
2094  
2095  
2096  
2097  
2098  
2099  
2100  
2101  
2102  
2103  
2104  
2105  
2106  
2107  
2108  
2109  
2110  
2111  
2112  
2113  
2114  
2115  
2116  
2117  
2118  
2119  
2120  
2121  
2122  
2123  
2124  
2125  
2126  
2127  
2128  
2129  
2130  
2131  
2132  
2133  
2134  
2135  
2136  
2137  
2138  
2139  
2140  
2141  
2142  
2143  
2144  
2145  
2146  
2147  
2148  
2149  
2150  
2151  
2152  
2153  
2154  
2155  
2156  
2157  
2158  
2159  
2160  
2161  
2162  
2163  
2164  
2165  
2166  
2167  
2168  
2169  
2170  
2171  
2172  
2173  
2174  
2175  
2176  
2177  
2178  
2179  
2180  
2181  
2182  
2183  
2184  
2185  
2186  
2187  
2188  
2189  
2190  
2191  
2192  
2193  
2194  
2195  
2196  
2197  
2198  
2199  
2200  
2201  
2202  
2203  
2204  
2205  
2206  
2207  
2208  
2209  
2210  
2211  
2212  
2213  
2214  
2215  
2216  
2217  
2218  
2219  
2220  
2221  
2222  
2223  
2224  
2225  
2226  
2227  
2228  
2229  
2230  
2231  
2232  
2233  
2234  
2235  
2236  
2237  
2238  
2239  
2240  
2241  
2242  
2243  
2244  
2245  
2246  
2247  
2248  
2249  
2250  
2251  
2252  
2253  
2254  
2255  
2256  
2257  
2258  
2259  
2260  
2261  
2262  
2263  
2264  
2265  
2266  
2267  
2268  
2269  
2270  
2271  
2272  
2273  
2274  
2275  
2276  
2277  
2278  
2279  
2280  
2281  
2282  
2283  
2284  
2285  
2286  
2287  
2288  
2289  
2290  
2291  
2292  
2293  
2294  
2295  
2296  
2297  
2298  
2299  
2300  
2301  
2302  
2303  
2304  
2305  
2306  
2307  
2308  
2309  
2310  
2311  
2312  
2313  
2314  
2315  
2316  
2317  
2318  
2319  
2320  
2321  
2322  
2323  
2324  
2325  
2326  
2327  
2328  
2329  
2330  
2331  
2332  
2333  
2334  
2335  
2336  
2337  
2338  
2339  
2340  
2341  
2342  
2343  
2344  
2345  
2346  
2347  
2348  
2349  
2350  
2351  
2352  
2353  
2354  
2355  
2356  
2357  
2358  
2359  
2360  
2361  
2362  
2363  
2364  
2365  
2366  
2367  
2368  
2369  
2370  
2371  
2372  
2373  
2374  
2375  
2376  
2377  
2378  
2379  
2380  
2381  
2382  
2383  
2384  
2385  
2386  
2387  
2388  
2389  
2390  
2391  
2392  
2393  
2394  
2395  
2396  
2397  
2398  
2399  
2400  
2401  
2402  
2403  
2404  
2405  
2406  
2407  
2408  
2409  
2410  
2411  
2412  
2413  
2414  
2415  
2416  
2417  
2418  
2419  
2420  
2421  
2422  
2423  
2424  
2425  
2426  
2427  
2428  
2429  
2430  
2431  
2432  
2433  
2434  
2435  
2436  
2437  
2438  
2439  
2440  
2441  
2442  
2443  
2444  
2445  
2446  
2447  
2448  
2449  
2450  
2451  
2452  
2453  
2454  
2455  
2456  
2457  
2458  
2459  
2460  
2461  
2462  
2463  
2464  
2465  
2466  
2467  
2468  
2469  
2470  
2471  
2472  
2473  
2474  
2475  
2476  
2477  
2478  
2479  
2480  
2481  
2482  
2483  
2484  
2485  
2486  
2487  
2488  
2489  
2490  
2491  
2492  
2493  
2494  
2495  
2496  
2497  
2498  
2499  
2500  
2501  
2502  
2503  
2504  
2505  
2506  
2507  
2508  
2509  
2510  
2511  
2512  
2513  
2514  
2515  
2516  
2517  
2518  
2519  
2520  
2521  
2522  
2523  
2524  
2525  
2526  
2527  
2528  
2529  
2530  
2531  
2532  
2533  
2534  
2535  
2536  
2537  
2538  
2539  
2540  
2541  
2542  
2543  
2544  
2545  
2546  
2547  
2548  
2549  
2550  
2551  
2552  
2553  
2554  
2555  
2556  
2557  
2558  
2559  
2560  
2561  
2562  
2563  
2564  
2565  
2566  
2567  
2568  
2569  
2570  
2571  
2572  
2573  
2574  
2575  
2576  
2577  
2578  
2579  
2580  
2581  
2582  
2583  
2584  
2585  
2586  
2587  
2588  
2589  
2590  
2591  
2592  
2593  
2594  
2595  
2596  
2597  
2598  
2599  
2600  
2601  
2602  
2603  
2604  
2605  
2606  
2607  
2608  
2609  
2610  
2611  
2612  
2613  
2614  
2615  
2616  
2617  
2618  
2619  
2620  
2621  
2622  
2623  
2624  
2625  
2626  
2627  
2628  
2629  
2630  
2631  
2632  
2633  
2634  
2635  
2636  
2637  
2638  
2639  
2640  
2641  
2642  
2643  
2644  
2645  
2646  
2647  
2648  
2649  
2650  
2651  
2652  
2653  
2654  
2655  
2656  
2657  
2658  
2659  
2660  
2661  
2662  
2663  
2664  
2665  
2666  
2667  
2668  
2669  
2670  
2671  
2672  
2673  
2674  
2675  
2676  
2677  
2678  
2679  
2680  
2681  
2682  
2683  
2684  
2685  
2686  
2687  
2688  
2689  
2690  
2691  
2692  
2693  
2694  
2695  
2696  
2697  
2698  
2699  
2700  
2701  
2702  
2703  
2704  
2705  
2706  
2707  
2708  
2709  
2710  
2711  
2712  
2713  
2714  
2715  
2716  
2717  
2718  
2719  
2720  
2721  
2722  
2723  
2724  
2725  
2726  
2727  
2728  
2729  
2730  
2731  
2732  
2733  
2734  
2735  
2736  
2737  
2738  
2739  
2740  
2741  
2742  
2743  
2744  
2745  
2746  
2747  
2748  
2749  
2750  
2751  
2752  
2753  
2754  
2755  
2756  
2757  
2758  
2759  
2760  
2761  
2762  
2763  
2764  
2765  
2766  
2767  
2768  
2769  
2770  
2771  
2772  
2773  
2774  
2775  
2776  
2777  
2778  
2779  
2780  
2781  
2782  
2783  
2784  
2785  
2786  
2787  
2788  
2789  
2790  
2791  
2792  
2793  
2794  
2795  
2796  
2797  
2798  
2799  
2800  
2801  
2802  
2803  
2804  
2805  
2806  
2807  
2808  
2809  
2810  
2811  
2812  
2813  
2814  
2815  
2816  
2817  
2818  
2819  
2820  
2821  
2822  
2823  
2824  
2825  
2826  
2827  
2828  
2829  
2830  
2831  
2832  
2833  
2834  
2835  
2836  
2837  
2838  
2839  
2840  
2841  
2842  
2843  
2844  
2845  
2846  
2847  
2848  
2849  
2850  
2851  
2852  
2853  
2854  
2855  
2856  
2857  
2858  
2859  
2860  
2861  
2862  
2863  
2864  
2865  
2866  
2867  
2868  
2869  
2870  
2871  
2872  
2873  
2874  
2875  
2876  
2877  
2878  
2879  
2880  
2881  
2

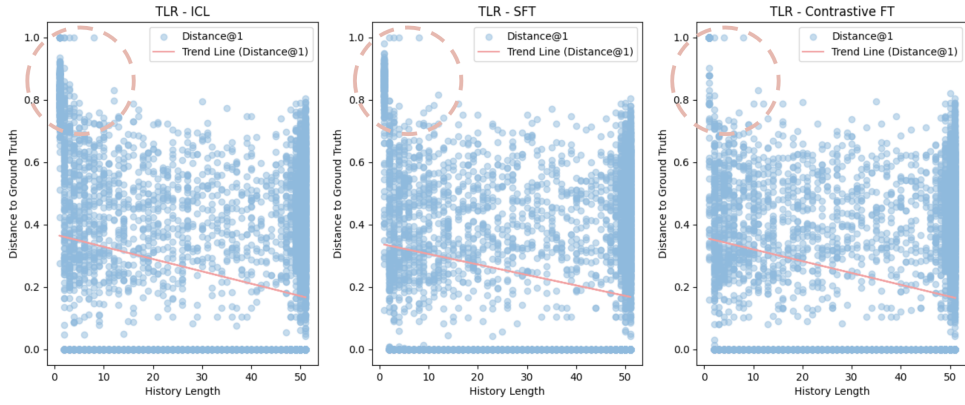


Figure 12: Semantic distance ( $\phi$ ) vs. history length on ICEWS14 under TLR sampling. The encircled region highlights CL's improved semantic grounding in sparse-history settings.

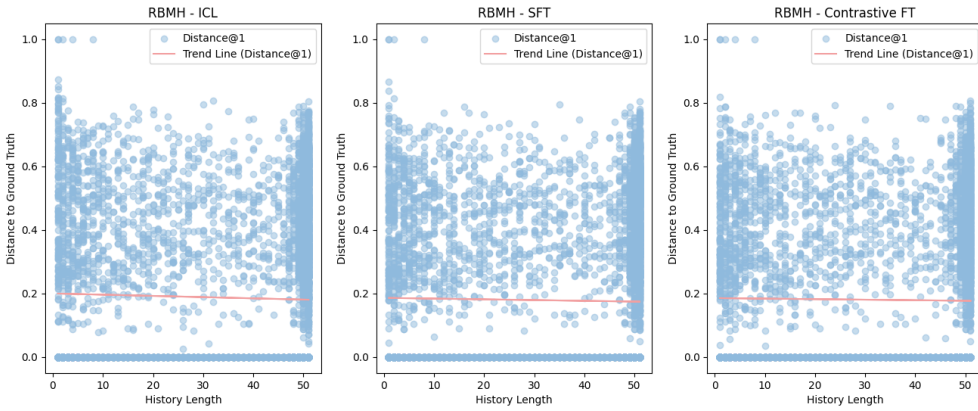


Figure 13: Semantic distance ( $\phi$ ) vs. history length for the same TLR-identified sparse samples, but evaluated under *RBMH Sampling*. The model exhibits more stable behavior across history lengths.

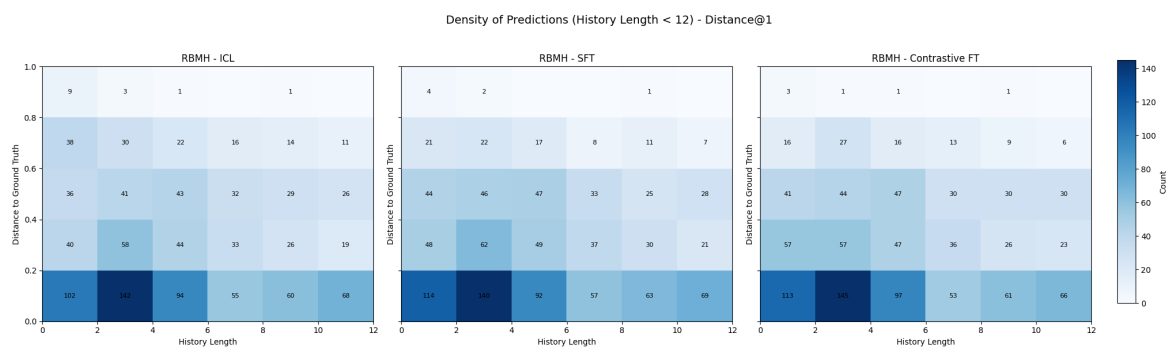


Figure 14: Semantic distance ( $\phi$ ) vs. history length for the same TLR-identified sparse samples, but evaluated under *RBMH Sampling*. CFT learns better with RBMH as it samples the deeper relationships between entities.

## Model Outputs

### ICL-LLaMA2-7b

1. Citizen\_(Nigeria)
2. Boko\_Haram
3. Suleiman\_Abba
4. Other\_Authorities\_/\_Officials\_(Nigeria)
5. Aliyu\_Mohammed\_Gusau
6. Nigerian\_Army
7. Nigerian\_Army
8. Nigerian\_Army
9. Nigerian\_Army
10. Other\_Authorities\_/\_Officials\_(Nigeria)

### RECIPE-TKG-LLaMA2-7b

1. Citizen\_(Nigeria)
2. Boko\_Haram
3. Suleiman\_Abba
4. Other\_Authorities\_/\_Officials\_(Nigeria)
5. Aliyu\_Mohammed\_Gusau
6. Government\_(Nigeria)
7. Military\_(Nigeria)
8. Abdul\_Aziz\_Yari
9. Chief\_of\_Staff\_(Nigeria)
10. Abdul\_Aziz\_Yari

### GenTKG-LLaMA2-7b

1. Citizen\_(Nigeria)
2. Boko\_Haram
3. Suleiman\_Abba
4. Other\_Authorities\_/\_Officials\_(Nigeria)
5. Nigeria
6. Aliyu\_Mohammed\_Gusau
7. Nigeria
8. Nigeria
9. Nigeria\_Army
10. None

### RECIPE-TKG-LLaMA3-8b

1. Citizen\_(Nigeria)
2. Other\_Authorities\_/\_Officials\_(Nigeria)
3. Boko\_Haram
4. Suleiman\_Abba
5. Defense\_/\_Security\_Ministry\_(Nigeria)
6. Terrorist\_(Boko\_Haram)
7. Employee\_(Nigeria)
8. Terrorist\_(Nigeria)
9. Senior\_Military\_Official\_(Nigeria)
10. Defense\_Personnel\_(Nigeria)

**Ground-truth entity:** High\_Ranking\_Military\_Personnel\_(Nigeria)

Figure 15: Top-10 predictions from four models. RECIPE-TKG produce semantically closer outputs to the ground truth.